HHS Public Access

Author manuscript

Angiogenesis. Author manuscript; available in PMC 2015 October 01.

Published in final edited form as:

Angiogenesis. 2014 October ; 17(4): 779–804. doi:10.1007/s10456-014-9440-7.

The chicken chorioallantoic membrane model in biology, medicine and bioengineering

Patrycja Nowak-Sliwinska[1,*], **Tatiana Segura**[2], and **M. Luisa Iruela-Arispe**[3,*]

[1]Institute of Chemical Sciences and Engineering, Swiss Federal Institute of Technology (EPFL), Lausanne, Switzerland [2]Department of Chemical and Biomolecular Engineering, UCLA, Los Angeles, USA [3]Molecular Biology Institute, UCLA, Los Angeles, USA

Abstract

The chicken chorioallantoic membrane (CAM) is a simple, highly vascularized extraembryonic membrane, which performs multiple functions during embryonic development, including but not restricted to gas exchange. Over the last two decades, interest in the CAM as a robust experimental platform to study blood vessels has been shared by specialists working in bioengineering, development, morphology, biochemistry, transplant biology, cancer research and drug development. The tissue composition and accessibility of the CAM for experimental manipulation, makes it an attractive preclinical *in vivo* model for drug screening and / or for studies of vascular growth. In this article we provide a detailed review of the use of the CAM to study vascular biology and response of blood vessels to a variety of agonists. We also present distinct cultivation protocols discussing their advantages and limitations and provide a summarized update on the use of the CAM in vascular imaging, drug delivery, pharmacokinetics and toxicology.

Keywords

angiogenesis; anti-vascular therapies; chicken chorioallantoic membrane; bioengineering; lymphangiogenesis; organ transplantation; physical forces; tumor vasculature

1. General information

1.1. Introduction

The visibility, accessibility, and rapid developmental growth of the chorioallantoic membrane (CAM) offer clear advantages to study and manipulate vascular functions. The first use of the system dates of 1911 when Rous and Murphy demonstrated the growth of

[*]Corresponding authors: M. Luisa Iruela-Arispe, Molecular Biology Institute, UCLA, 615 Charles E. Young Drive South, Los Angeles, CA 90095, USA, Tel: +1 310 794 5763, Fax: +1 310 794 5766, arispe@mcdb.ucla.edu; Patrycja Nowak-Sliwinska, Institute of Chemical Sciences and Engineering, Swiss Federal Institute of Technology (EPFL), Lausanne, CH-1015, Switzerland; Tel: +41 21 693 5169, Fax: + 41 21 693 5110, Patrycja.Nowak-Sliwinska@epfl.ch.

Conflict of interest

The authors declare that they have no conflict of interest.

chicken sarcoma tumors transplanted onto the CAM [1]. One year later, Murphy published successful heterologous transplantations of tumors in this model [2].

In 1930s the CAM was first exploited for cultivation of viruses and bacteria [3–5]. Its application in vascular-related questions occurred only several decades later, but it quickly gained recognition as an excellent model system for studies associated with vascular responses.

The initial vascular-related experiments employed grafts from tumors [1,2] and later methylcellulose discs in which compounds were encapsulated to determine induction of vessel growth or inhibition by morphological criteria [6–8]. These discs provided a venue for the slow release of pro- or anti- angiogenic factors and thus, a “high” throughput platform for therapeutic exploration emerged. Problems with this method were associated with the difficulty in distinguishing the *existing* from the *newly-formed* (or induced) capillaries. In addition, the methylcellulose discs by itself could, on occasion, induce angiogenesis even in the absence of growth factors, particularly if crystals of salt were present. Thus, the approach was subsequently replaced by 3D models of vascular invasion and other alternatives [9,10].

In addition to angiogenesis screens, the CAM has been used to explore hemodynamics, immune cell trafficking, transplantation and responses to therapy. In this review we will provide a comprehensive summary of the use of this model to study vascular-related questions bringing into this description a rigorous evaluation of the pros and cons.

1.2. Structure and development of the CAM

The CAM develops in a similar manner as the allantois in mammals as it extends extra embryonically from the ventral wall of the endodermal hind-gut (Figure 1). However, in birds it also fuses with the chorion to form the chorioallantoic membrane. Initially avascular, it quickly gains a rich vascular plexus (Figure 2a,b) that rapidly acquires hierarchic complexity with the emergence of arteries and veins (Figure 2c). The growth of the CAM occurs from embryonic development day 3 (stage 18 of Hamburger and Hamilton, [11]) and it is completed by day 10 (Figure 3) however, it is only fully differentiated by day 13. This growth requires impressive rates of cell division with short cell cycles. While this has not been significantly explored, bromodeoxyuridine (BrdU) incorporation revealed rapid cell cycles and extensive proliferation (Figure 4).

The CAM functions as the respiratory organ of avian embryos. Although most of attention is given to the vascular system, it is important to emphasize that the CAM has a fully developed lymphatic system that holds remarkable functional and molecular similarities to mammalian lymphatics [12]. A more detailed description of lymphatic development in the CAM will be presented later in the review.

Histologically, the CAM consists of two epithelial sheets that limit a thin layer of stroma (Figure 5). The upper epithelium is of ectodermal origin, while the stroma and the lower epithelium are of mesodermal and endodermal origin respectively. It is within the stroma that the blood vasculature and lymphatics reside. In this manner, it is important to realize

that any compound delivered on the surface of the CAM has to pass across the surface epithelium and reach the vessels in the stroma. Poor humidity conditions when the CAMs are cultured *ex ovo* induce significant cell division and keratinization of this upper, and normally single, epithelial layer; making it even more difficult to deliver soluble molecules to the underlying vascular tree. Therefore the humidity status is critical during the experimental use of this system.

It is important not to mistake the CAM with the yolk membrane, which is also highly vascularized. This second membrane is associated with the yolk and it has distinct properties. Figure 1 clearly shows both membranes, that are easily distinguishable in the young embryos and less noticeable in an older embryo (Figure 1). In the egg, the CAM attaches to the surface of the egg shell, removing calcium and obtaining oxygen for the atmosphere across the porous shell. The attachment of the CAM to the shell inner membrane occurs shortly after fertilization (day 4–5) and thus, opening fertilized eggs for cultivation has to be done by day 3, as after this time, rupture of the shell is associated with rupture of the CAM. Also when opening small windows for application of compounds at latter time points, meticulous dissection of the shell and its underlying membrane is necessary to expose the vascular CAM without damaging small vessels.

1.3. Advantages and disadvantages of the CAM model

As already stated, the CAM model offers multiple advantages over other *in vivo* models used to study angiogenesis and vascular biology. The most prominent advantage of the model is its accessibility and rapid growth (see Table 1). The CAM develops in a short time from a small avascular membrane into a structure that covers the entire inner surface of the shell displaying a densely organized vascular network. This process occurs over a period of only 7 days (day 3–10). It is this enormous angiogenic boost provides a wealth of information related to required developmental pathways. In addition, this model can also be used to study pathological processes by simple exposure to cytokines, hormones or drugs, or by transplantation of tissues, isolated cells or materials.

The great accessibility of the CAM and the easy handling of the model for both intervention and imaging of the vasculature have attracted many researchers. In particular, the broad applicability of distinct imaging modalities that range from microscopic- to magnetic resonance- to positron emission tomography imaging (MRI and PET) offer multiple benefits. In addition, due to the transparency of its superficial layers, nearly any wavelength in the visible part of the electromagnetic spectrum can be used for fluorescence imaging. For applications related to transplantation, an important benefit is the slow developmental progression of the immune system that reaches physiological activity only by day 15 post-fertilization [13]. Thus, unwanted immunological reactions are limited, facilitating the transplantation of xenogeneic tissues, e.g. human tumors.

Last but not least, the cost-effectiveness of the model adds to the long-list of benefits. In fact, the price of a fertilized egg is 100 times lower than that of a mouse of a common strain.

Nonetheless there are also limitations. Perhaps the most prominent being the limits on the number of reagents compatible with avian species, including antibodies, cytokines and

primers which might not work in chick tissues. Along these lines, genetic manipulation, albeit possible through virus, it is not as “easy” as in mice.

The CAM contains already a well-developed vascular network, which makes it difficult to discriminate between new capillaries and already existing ones. Another limitation is that if experiments extend after 15 days, a non-specific inflammatory reaction can occur that may limit the success of grafting. Such reactions may provoke angiogenic responses, which are difficult to distinguish from an angiogenic activity of grafted material [7].

1.5. Cultivation protocols

Several protocols are available for culturing avian embryos. The type of experiment to be conducted directs the choice of the protocol. In many cases, investigators rupture the egg and transfer the embryo to a 10 cm petri dish at day 3 post-fertilization. This *ex ovo* culture of the embryo, also called shell-less embryo culture offers ample observation and manipulation space, allowing for testing of several samples in a single CAM. For this approach, the eggs are first kept at 38°C in a humidified incubator (days 0–3) on the side to ensure the position of the embryo is opposite to where the cracking of the shell occurs. Subsequently, a small whole is made on the side of the air chamber to equilibrate pressure and the egg is cracked into a petri dish. Naturally, the exposure of the entire embryo and yolk requires sterile conditions. Also removing the embryo from the shell is associated with a low survival rate, due to the frequent rupture of the yolk membrane either during or after culture. This occurs due to excessive distension of the yolk in the flat dish (Figure 1b) [8,6]. *Ex ovo* survival rates can be drastically improved through reducing the impact during the cracking of the egg shell and placing the embryo in a confined curved space rather than a flat petri dish for culture. Gentle cracking of the egg can be achieved using a circular saw rather than cracking the egg against a sharp edge (Figure 8a). Alternative cultivating dishes include large weight boats (Figure 8b) and plastic inserts that can be placed inside 100 mm petri dishes to introduce a curvature to the dish (Figure 8c). In addition, it is paramount to keep the humidity in the incubator at 98% or higher and to maintain the culture environment sterile. Using these approaches the viability is around 50% at day 14. For a demonstration of a refined chick *ex ovo* culture and CAM assay with survival rates over 50% refer to the video article of Dohle et al, [14].

In ovo cultivation is an important alternative that improves significantly the survival of the embryos. Fertilized eggs are transferred to the incubator equipped with an automatic rotator for three days. Turning prevents the embryo from sticking to the shell membranes, as it would if it is left in one position too long. Good results can be obtained by turning the eggs the first thing in the morning, again at noon, and the last thing at night. Alternatively, the use of an automatic rotator enables slow but constant movement of the eggs.

The process of *in ovo* cultivation is initiated also at day 3 post-fertilization. At this time, a hole of approximately 3 mm in diameter should be created in the eggshell with a sterile tweezers and covered with a laboratory wrapping film to prevent dehydration and possible infections (Figure 8d). The eggs are then returned to the incubator with a relative air humidity of 65% and a temperature of 37°C in a static position until use (Figure 8e). This initial small incision changes the pressure inside the egg and prevents binding of the CAM

with the shell membrane. At day 7 or later, the hole is extended to a diameter of approximately 3 cm in order to provide access to the chorioallantoic membrane (Figure 8f). This approach still enables experimentation through a window and it offers an almost unchanged physiological environment for the developing embryo.

Depending on the country and regulations that provide oversight to the use of animals, avian embryos are allowed to develop until the hatching stage, usually at day 21 after fertilization. This cultivation protocol has been used broadly e.g. to study vascular development and (pro/anti) angiogenesis, tumor growth and metastatic progression, and to evaluate the effect of chemo-, radiation-, and photodynamic therapies, see Table 2.

2. CAM as a screening platform

The CAM has served as an *in vivo* platform for experimentation for more than 50 years. This system has been used for the study of vascular development and angiogenesis, tumor growth and metastasis [32], respiratory properties [33], ion transport [34,35], selective vascular occlusion therapies, biocompatibility of engineered materials, drug distribution and toxicology. Next we review this literature and delve into the methodology used to provide readers with choices for future experimentation.

2.1. Vascular development and angiogenesis

As previously discussed, because of its rapid vascular growth, the CAM has been the model of choice to evaluate the effect of a wide number of compounds on growing vessels. Many pro- and anti-angiogenic agents have been tested by quantifying the morphological responses of the CAM vasculature. These compounds have included growth factors [6,36], hormones [37,38], natural molecules, anti-cancer agents [39], gases [40], organometallic compounds [41–43], pro-angiogenic molecules [37], antibiotics [44], antibodies and synthetic small molecules [45,36,7,46]. The efficacy of such compounds has been evaluated using both qualitative and quantitative methods based on the assessment of the vascular morphology and density. Initially, this was done by scoring the extent of vascularization on a graded scale of 0–4 [47]. Alternatively, vascular growth was also assessed by quantifying the number of vessels that invaded, against gravity, an avascular matrix in which pro-angiogenic compounds were casted (Figure 9a–c) [10,9]. Injection of either fluorescent compounds or contrasting agents (india ink) favored visualization and eased the quantification (Figure 9d).

More recently, a number of attractive imaging techniques (Table 3) were applied to the CAM to facilitate visualization and offer objective quantification. Even MRI and PET imaging have been used, but the resolution of these techniques might not be sufficient for the identification of vascular structures (Figure 10).

Several visual vessel-counting methods [61] or automated approaches [62–64] have been also developed (Table 4). Quantification, has frequently relied on descriptors such as vascular density [62,65], vessel branching points/mm^2 [66,64], vascular length [67], or endpoint density/mm^2 [68,69], see Table 4. An example of automatic *in vivo* and *in ovo* quantification technique developed by Nowak-Sliwinska et al. is presented in Figure 11.

Gene expression profiling associated with the physiological CAM development [70], as well as with the angiogenic switch during experimental tumor progression [71] has been reported, but the lack of initial sequence information for the chick has limited the use of this more molecular approach. Instead these types of studies have accelerated more in the retina (77).

2.2. Lymphangiogenesis

Lymphangiogenesis in the CAM emerges during mid-development (days 5–9 post-fertilization) following the initial growth of the blood vascular system and via expansion of blind-ended sprouts [79]. Isolated lymphatic endothelial progenitor cells are recruited to the tips of growing vessels and grafting quail-chicken chimera experiments showed unequivocally that the allantoic mesoderm has lymphangiogenic potential [12]. Concurrent to haemangiogenesis expansion, lymphatic vessels enlarge and split offspring vessels, accompanied by transient capillary expression of alpha smooth muscle actin (SMA) and recruitment of polarized mural progenitor cells. VEGF-A and hepatocyte growth factor (HGF) are well known angiogenesis inducers in normal and pathologic conditions. Cimpean et al. showed that VEGF-A/HGF combination was able to promote a strong angiogenic response and expression of prospero homeobox protein 1 (Prox1) in the lymphatic endothelial cells of the CAM [80].

The lymphatics of the chorioallantoic membrane (CAM) are drained by lymphatic trunks of the umbilicus that are connected to the posterior lymph hearts. Intra-embryonic lymphatics are drained via paired thoracic ducts into the jugulo-subclavian junction. Similarly to mammalian lymphatics, the lymphatics of the CAM are characterized by an extremely thin endothelial lining, pores, and the absence of a basal lamina [81]. Molecularly, and in analogy to the mammalian system, lymphatic endothelial cells in the CAM are characterized by the expression of VEGFR-2 and -3 and are also Prox1 positive. Application of VEGF-C, the ligand of these two receptors, on the differentiated CAM, induces proliferation of lymphatic endothelial cells and formation of enlarged lymphatic sinuses. Under normal development, the sources of VEGF-C are the allantoic epithelium and the wall of the larger blood vessels. The fact that the lymphatics of the CAM travel along the side of the larger blood vessels (Figure 6) indicate that the high level of VEGF-C from the wall of these vessels contributes to pattern the normal distribution of lymphatics in the CAM. The presence of a lymphatic system in the CAM opens the possibility of studying its function and response to a large number of compounds. Lymphatics have been shown to remodel in response to pathological conditions and play a critical role in tumor metastasis [82]. Papoutis et al. studied the effects of two rat tumor cell lines (C6 glioma and 10AS pancreatic carcinoma) that differ in their VEGF-C expression profiles [83]. Whereas the 10AS cell line expresses high levels of VEGF-C, the C6 glioma cells only weakly express VEGF-C. They showed that only the 10AS cells induce lymphangiogenesis.

2.3. Assessment of vascular permeability, tumor growth, and metastasis

2.3.1. Vessel permeability—The permeability of the vasculature can be assessed in real-time using the traffic of fluorescent dextrans of various molecular weights i.e. macromolecular drug carriers (70 kDa) and antibodies (150 kDa) into the tumor interstitial space. Whereas large dextrans of 2000 kDa are sequestered within the lumen of the tumor

vasculature [84,85]. These alternative sizes of dextrans offer real-time monitoring power to study vascular leak in the CAM vasculature during the sequential development phases of endothelial proliferation (angiogenesis), cytodifferentiation and senescence [86–88]. It also provides the ability to determine the pharmacodynamics and pharmacokinetics of drugs diffusing from the CAM vasculature [89] or in response to engrafted tumor explants [85]. Regional and temporal differences in vessel permeability within the tumor microenvironment may also be captured at high resolution using an intravital imaging approach.

An enhancement of the vascular permeability in the CAM has been studied using VEGF [90] or techniques such as low-dose photodynamic therapy [20] or a low-frequency contrast material-enhanced ultrasound on the vascular endothelium [91]. In the latter studies diameter of affected vessels, number of extravasation sites, extravasation rate, area, and location, as well as changes in endothelial cells and basement membrane were evaluated.

2.3.2. Tumor growth, and metastasis—During past three decades several studies have reported successful use of the CAM in cancer biology and tumor angiogenesis (Table 5). The first report of an angiogenic response in the CAM was induced by Jensen Rat Sarcoma and was described in 1913 by Murphy [92]. To date many tumor cells placed on the CAM have been shown to engraft and follow all steps of tumor progression: grow, angiogenesis, invasion, extravasation and metastasis. The spontaneous metastatic events occurring after cell inoculation or intravasation into the vasculature has provided valuable information to understand tumor progression and metastatic potential of specific cell lines / primary tumor fragments.

Table 5 summarizes the cell types successfully grown on the CAM. Moreover, the vascularization of neoplastic and normal tissue fragments, either fresh or cryopreserved, grafted on the CAM has been evaluated in detail [71].

The highly vascularized network of the CAM sustains tumor viability and within a few days after cell grafting (Figure 7) it can offer the means to study intravascular invasion of tumor cells *in vivo* [107,23,73]. In fact, trafficking of tumors cells in the chicken embryo has been shown by real-time imaging [73]. Furthermore, since the CAM is an isolated system, the half-life of many molecules such as small peptides tends to be much longer in comparison to mammalian models, allowing study of potential anti-metastatic compounds that are only available in small quantities [73,93]. Table 6 summarizes tumor types shown to metastasize in the CAM.

Another mechanism of cell dissemination that takes place along the blood vasculature is called vasculotropism. In this process tumor cells appear to grow along the existent blood vessels, rather then randomly distributed within the CAM mesoderm. This was shown for human HT-1080 fibrosarcoma [110], human A2780 ovarian carcinoma (Nowak-Sliwinska P, unpublished data), and human melanoma [113].

2.4. Selective anti-vascular therapies and diagnosis

2.4.1. Photodynamic therapy—The well-vascularized surface of the CAM has several advantages as a model for studying the vascular effects of photodynamic therapy (PDT). PDT is based on the interaction of a systemically or topically applied photosensitizing agent (photosensitizer, PS) with molecular oxygen after irradiation with light of an appropriate wavelength [114]. The initial reaction, leading to generation of reactive singlet oxygen, activates a cascade of chemical and physiological responses, which results in a temporary or permanent occlusion of the irradiated vasculature [115]. The angio-occlusive effect of PDT in the CAM has been has been monitored and described in detail by Debefve et al. [51].

Various light sources [29] and different types of photosensitizers have been tested on the CAM model [116–119] enabling the comparison between different treatment conditions. The photosensitizers can be administrated in the CAM intraperitonealy [120], topically [121] or, most often, intravascularly [42,18,117,122,20,116]. Since the photosensitizers are usually hydrophobic, to facilitate its administration, they are distributed in the form of liposomes [123][117], biocompatible solvents like N-methyl-pyrrolidone, as well as 0.9% sodium chloride [124]. In addition, polymeric nanoparticles were also used for this purpose (e.g. poly(lactide-co-glycolide, PLGA or PLA) [118]. An overview of delivery systems tested on the CAM is listed in Table 7. PDT is known to provoke an angiogenic response [115]. Therefore its combination with a variety of topically [140,42,19,141,142] or intravenously administered [32] anti-angiogenic compounds have been studied using the CAM for their ability to suppress vascular growth.

The CAM was also exploited to determine the relationship between the progression between tissue oxygen concentration during PDT and the resulting vascular damage. Measuring the local pO2 is also of interest for other types of treatments, such as radiotherapy or photodynamic therapy, as it is well established that tissue oxygenation plays an important role on the outcome of such treatments. The measurements of the pO2 in the CAM was performed, using a micro-O2-electrode [143], the delayed fluorescence [121] or luminescence quenching of a ruthenium derivative [144] monitored with a dedicated optical, fiber-based, time-resolved spectrometer or a fiber-optic oxygen sensor [32].

Low-dose PDT enhances vessel permeability, therefore might be used as a drug delivery method [145]. The perturbation of endothelial cell membranes by PDT results in the loss of tight junctions responsible for the sealing properties between adjacent cells, and consequently leaving enlarged gaps between cells that increase the vascular permeability to macromolecules following PDT. This principle is currently being applied for targeted delivery of chemotherapy, as the injection of a reduced amount of a chemotherapeutic drug could be effective due to enhanced local delivery rendered possible by combining Visudyne®-PDT with aspirin [86].

2.4.2. Photodynamic diagnosis—Photodynamic diagnosis (PDD) of cancer using photosensitizers is one of the major advances as a new technique for early cancer detection. The clinical application of hypericin (HY) or aminolevulinic acid (ALA) and its derivative Hexvix® has been demonstrated to improve visualization of urological cancers as compared to white light cystoscopy [146]. This light-induced fluorescence after treatment is an

experimental model used in the early diagnosis of cancerous disorders in urology. Malik et al. conducted an *in vivo* study evaluating the ALA-based fluorescence diagnosis of endometric implants on the CAM [147]. Saw et al. reported on the hypericin-N-methyl pyrrolidone (HY-NMP) formulations in the CAM inoculated human bladder cancer cells as a potential fluorescence diagnostic agent [148]. The NMP formulations investigated were able to produce significantly higher contrast for tumor tissues and at earlier time points than was possible with HY in albumin. MPEG-hexPLA micelles were successfully used as hypericin carriers for ovarian cancer diagnostics [149].

2.4.3. Laser photoangiolysis—Selective vascular ablation (photoangiolysis) using pulsed lasers that target hemoglobin is an effective therapeutic strategy for many lesions residing in the thin tissue that forms the vocal folds. However, vessel rupture with extravasation of blood reduces selectivity for vessels, which is frequently observed with the 0.45-ms, 585 nm pulsed dye laser. The CAM has been useful predicting the effects of photoangiolytic lasers on the vocal fold microvasculature. Specifically, the CAM has been explored to test the effects of distinct laser settings, modes of delivery, active cooling, and wavelengths. Such information has been essential for optimizing the effectiveness of lasers in treating laryngeal pathology while preserving vocal function. One example is the 980 nm Gold laser that achieved selective vessel coagulation [150]. In other study, the pulsed 532 nm potassium-titanyl-phosphate laser was used to achieve selective vessel destruction without rupture using the CAM under conditions similar to flexible laryngoscopic delivery of the laser in clinical practice. It was shown that this treatment was effective for ablating microcirculation while minimizing vessel wall rupture and hemorrhage [151].

2.4.4. Radiotherapy—A few reports have used the CAM in radiotherapy-related studies. Interestingly, chicken embryos are able to tolerate high dose of X-rays under single or multifractionated irradiation, an obvious advantage for these studies. Not surprisingly X rays have been shown to decrease the number of blood vessels, most probably due to vascular targeting within the first hours after irradiation [152]. However, it appears that X-rays promote multiple effects in the CAM: (i) induce early apoptosis of CAM cells, a property that can be exploited to screen radioprotective compounds [153], (ii) modulate the synthesis and deposition of extracellular matrix proteins involved in regulating angiogenesis and (iii) affect angiogenesis induced by tumor cells implanted onto the CAM [154]. More recently, the CAM/embryos has been used to test the activity of radiosensitizers. For example, etanidazole, a well-known hypoxic cell radiosensitizer, was evaluated using tumor-bearing chick embryos [21].

Distinct modalities of X-ray beams have also been evaluated in the CAM. In particular, microplanar beams (microbeam radiation, MR) have been compared to broad beams (seamless radiation) [155]. MR promotes capillary damage, with tissue injury caused by insufficient blood supply. Vascular toxicity and physiological effects of MR depend on the stage of capillary maturation and appear within the first hour after irradiation. The authors noticed a dose dependent vacuolization of endothelial cells as well as growth retardation, resulting in a remarkable reduction in the vascular endpoint density. Finally, several preclinical studies in the CAM have used combination therapy and demonstrated an

increased effectiveness when radiotherapy is combined with an anti-angiogenic treatment [156,157].

Combined effects of paclitaxel and single or fractionated doses of ionizing radiation during angiogenesis were also evaluated [22]. X-rays suppression of angiogenesis includes anti-proliferative action and induction of nitric oxide (NO) which also inhibits vascular growth [158]. These results suggested that NO is involved in the anti-angiogenic mechanism of X-rays and that pharmacological manipulation of NO may offer an alternative therapeutic approach for treating pathological conditions involving angiogenesis [159].

2.4.5. Vascular disrupting agents—Vascular disrupting agents (VDA) that destroy irregular tumor blood vessels often exhibit an immediate impact on the vasculature of tumors provoking their collapse after a few applications. They are usually small molecule compounds that bind to the colchicine binding site of tubulin and cause extensive cytoskeletal rearrangements of the microtubules and the actin bundles in endothelial cells [160,161]. Disruption of small blood vessels, as well as hemorrhages as a result of leaking or broken vessels were observed shortly after administration of VDAs, e.g. verubulin [162], or the microtubule-depolymerizing agent C9 [163]. Moreover, the growth of solid tumors on the surface of the CAM was successfully inhibited by VDAs, e.g. phenyl-3-(2-chloroethyl) urea [164]. New compounds with both, anti-angiogenic and vascular-disrupting properties have been also frequently tested in the CAM model (i.e. deoxypodophyllotoxin [165], vinblastine [166], combretastatin A-4 or its gold derivative [167]).

2.5. Drug delivery systems, drug pharmacokinetics and biodistribution

Drug delivery systems (DDS) aim to distribute therapeutic agents to specific sites of injury or disease. Research on DDS includes: (i) the direct modification of the therapeutic agents to form drug conjugates, (ii) the encapsulation of the therapeutic agents into micro or nanosized structures, and (iii) the encapsulation or conjugation of the therapeutic agents into scaffolds. Most commonly, these different DDS are studied *in vitro* with cells in culture and then tested in pre-clinical animal models. However, the leap from *in vitro* cultured cells *to in vivo* pre-clinical animal models often leads to unsatisfactory performance which is frustrating due to the high cost of the pre-clinical studies. The CAM has been an excellent platform to test multiple DDS formulations concurrently, thus it has been used as an intermediate step between *in vitro* analysis and *in vivo* pre-clinical evaluation in mammals [168].

2.5.1. Pro-angiogenic drugs—In tissue repair, the controlled induction of angiogenesis directed at afflicted sites (ischemic tissue) is of great importance. To test the pro-angiogenic activity of different DDS, investigators frequently apply them directly onto the CAM surface and proceed to monitor the angiogenic response. These pro-angiogenic agents can be delivered as drug conjugates, as micro or nanoparticles, or as part of a tissue scaffold. For example, the delivery of growth factors such as VEGF121, VEGF165, and FGF-2 to induce an angiogenic activity has been extensively studied [36,6,128,136]. Using the CAM assay, researchers have been able to screen different formulations to find that the individual delivery of each of these factors entrapped within a matrix results in the formation of highly

leaky vessels [169], whereas the delivery of combinations of these factors or the immobilization of VEGF (either 121 or 165) yields vessels with normal morphology and adequate barrier performance (non-leaky vessels).

2.5.2. Anti-angiogenic drugs—The efficiency of formulations containing anti-angiogenic drugs with the CAM model may be easily evaluated by determining degree of vascular occlusion [125,56,30]. Efficacy of paclitaxel, delivered via various types of formulations, was studied on the CAM and elegantly reviewed by Vargas et al. [170]. Recently, surface-engineered dendrimers were used for tumor specific delivery of doxorubicin hydrochloride [138]. The later system enabled an initial rapid release followed by sustained release of doxorubicin hydrochloride with significant anti-angiogenic activity. Tetrac (tetraiodothyroacetic acid) covalently linked to poly (lactide-co-glycolide) as a nanoparticle arrested tumor-related angiogenesis and human renal cell carcinoma growth in the CAM model [131].

2.5.3. Biodistribution—Drug pharmacokinetics can be assessed using the blood sampling or selected organ extraction of fluorescence detection (in case of fluorescent drugs). The later method is widely used with direct fluorescence measurements in the CAM vasculature *in vivo* [20] or in *ex vivo via* tissue fluorescence analysis [171]. Due to the small organ size and low blood volume, both development-stage dependent [172] sensitive analysis methods should be used. Consequently, non-invasive methods such as biosensors (e.g. glucose [139]) for the analysis of drug concentration can be advantageous in this model.

2.6. Gas/ion transportation

As previously alluded to, the CAM functions as “the lung” of the avian embryo, and thus, it is responsible for gas exchange, but it also provides calcium transport from the eggshell into the embryo, it offers acid-base balance, and it mediates regulation of water, and electrolyte resorption from the allantoic cavity where urinary waste products are discharged.

The CAM is involved in the transport of sodium and chloride from the allantoic sac and calcium from the eggshell to the vasculature. Through dilation of the associated blood vessels (known as chorioallantoic vessels), the embryo is able to thermo-regulate and avoid overheating for long periods of time. Several studies related to gas and water exchange have been reported. For example, the functional role of hypoxia in vascular flow was nicely explored in the studies published by Lindgren and colleagues (128). Initially, the CAM performs gas-exchange functions via the area vasculosa, the main respiratory organ before day 6 [173], but this is gradually substituted by the CAM vessels. By day 14, the CAM capillary network is completely developed and by day 19 the embryonic lung ventilation starts as the CAM degenerates and the embryo hatches. Lindgren et al., showed that a one-time change in oxygenation of the external microenvironment between day 15 and day 19, could affect blood flow. Local hypoxia yield direct vasoconstriction, increasing the flow [174], demonstrating that ventilation is associated with perfusion.

In terms of calcium, the chorionic epithelial cells transport Ca2+ to the embryonic circulation at an impressive rate: 100 nmoles of calcium per hour for 1 cm2 of the CAM surface. The mechanism of this transport seems to rely on the sequestration of calcium

within endosome-like vesicles upon the initial uptake phase [94]. Interestingly, *in vitro* CAM ectodermal cells exhibit faster calcium influx rates when compared to human erythrocytes suggesting alternative calcium entry mechanisms [175]. This unidirectional process was shown to be highly specific for Ca2+ and regulated by vitamins D and K [176]. A detailed review of transepithelial ion transport through the chorionic epithelium has been described elsewhere [35].

2.7. Allergenicity and toxicity

The worldwide objection to the use of animals in testing of irritants and cosmetics makes the development of a system that does not use mammals highly desirable. Below are some important examples.

2.7.1. Skin irritation—A number of *in vitro* methods to assess skin and eye irritation/corrosion have been developed as alternatives to the *in vivo* rabbit tests [177]. Human skin models, like EpiSkin™ and SkinEthic™, that closely mimic the biochemical and physiological properties of the upper parts of the human skin, have undergone extensive formal validation and acceptance procedures in order to be broadly applicable. In Europe, the CAM and the cornea pocket assay have also been accepted for this purpose. In the CAM, potential for irritation can be assessed with specific read-outs on the membrane and/or vessels (hemorrhage, lysis, coagulation, changes small vessel diameter [178]), which is then compared to the effect of 5% sodium magnesium lauryl-myristyl-6-ethoxysulphate [178].

The chimeric skin-CAM system serves as a promising alternative to current animal-based sensitization approaches, particularly when using human grafts. The first report of a successful human skin graft onto the CAM was described by Goodpasture [58]. An important advantage of the CAM on skin engrafts as compared to *in vitro* models of organotypic skin explants is that the skin is maintained in a more “physiological status”, meaning dependent on vessels for its oxygenation. By having a continuous blood supply, the grafted skin remains viable for the same length of time as chick embryo survival. Furthermore, epidermal Langerhans cells (LC) are retained in the epidermis for several days after grafting into the CAM, unlike in organotypic explants [179]. Slodownik et al. used allergens to evaluate the LC as a measure of their allergic potency. All agents with known allergic potential induced statistically significant migration of LC [180].

2.7.2. Eye irritation—Ocular tissues, such as the cornea and conjunctiva, are susceptible to injuries and adverse effects, either from administered drugs or additives used in pharmaceutical products [181,182]. Assessment of the toxicity of ophthalmic formulations and the potential for ocular irritation represents an essential step in the development of new ocular delivery systems. The CAM has replaced the highly controversial “Draize eye irritancy test” used to determine the irritation potential of cosmetics by placing liquid, flake and powdered substances into the eyes of rabbits. The hen’s egg test (HET-CAM) provides a platform for conjunctival irritation testing, as it responds to irritant substances with an inflammatory reaction similar to that seen in conjunctival tissue [183–185]. Various studies included classification of several classes of irritants, ranging from non-irritant to severe, with high correlations between the systems. This development was encouraging since it

suggested that *in vitro* models could provide valid alternatives for prediction of ocular toxicity [186]. After the application of the test substance (e.g. cholesterol or naltrexone), blood vessels are examined for irritant effects at different time points post-application. The evaluation includes assessment of hyperaemia, hemorrhage and clotting [187]. A time-dependent numerical score is then attributed to each test substance or formulation, to give an irritation score that ranges from slight to severe [187,188]. A modification of the HET-CAM assay was introduced by Hagino et al. [189] who used trypan blue to determine degree of cell death. Trypan blue has been used in many biological systems to distinguish between living and dead cells. As the amount of trypan blue adsorbed by the CAM can be measured spectrophotometrically, the quantification is simple and reproducible. When compared by simple linear regression, the degree of trypan blue adsorbed by the CAM and that obtained from Draize eye irritation test in the cornea presented high correlation coefficients, indicating that the CAM can be an excellent choice for predicting corneal injury without compromising quality.

The CAM has also been used as a model in surgical retinal research [190]. In fact, several of the new surgical tools, techniques for coagulating retina, microinjection, cannulation techniques, and endoscopic surgery were first tested in the CAM and subsequently evaluated in animal models. Microrobots that are used for intravitreal delivery of as well as other surgical applications were first evaluated on the CAM [191] prior to further testing into a rabbit eye [192].

2.8. Organ transplantation and tissue engineering

Due to its immunodeficiency prior to day 15 post-fertilization [13], the CAM has been extensively used to evaluate allogeneic and xenogeneic transplantations. In fact, the CAM is considered as a suitable model to study the implantation/biocompatibility process and to explore differentiation of tissue implants. It has also been used to evaluate tissue remodeling within or in response to the implanted material, regeneration events, and neovascularization. These processes depend on the mechanical and physico-chemical properties of the implanted material [178]. Already in 1916, for the first time, multiple chicken tissues were grafted in the chicken embryos [193]. More recently, allogeneic and xenogeneic tissues were successfully grafted on the CAM, such as liver [194], proliferative endometrium [195], adrenal gland or cerebellum [196], or intact human skin [58,179], see Table 8.

Transplanted tissues can survive and develop in the CAM by either peripheral anastomoses between implanted graft and original CAM vasculature or by new angiogenic growth from the CAM into the transplant. It has been demonstrated that the formation of peripheral anastomoses between pre-existing donor and host vessels is the most common, mechanism involved in the revascularization of embryonic grafts [71]. The assembly of graft and CAM blood vessels occurs between relatively large arteries or veins, resulting in chimeric vessels of varying morphology [203].

The CAM has been also used in stem cell research in which various extracellular matrices or synthetic polymer-derived scaffolds have been evaluated in an effort to construct desired tissue-like structures [173,198] [176]. The combination of biocompatible materials and stem

cells appears to be a future trend that might prove fruitful in comparison to other systems, in large part, due to the neovascular properties of the CAM.

To date tissue engineering has been successful in producing simple avascular tissues, such as skin and cartilage, which are thin enough for oxygen and other nutrients to diffuse passively. To sustain a tissue with large dimensions (greater than 400 μm in thickness), a vascular supply that effectively permeate the implant is essential [204]. However, caveats are also inherent to the system. In particular, inflammation and ulceration might occur in response to implants of non-biological materials. The next generation of tissue engineering products has been largely designed to promote timed release of growth factors and to achieve biocompatibility without promoting inflammation. Moreover, several technologies have been used to evaluate the biocompatibility and/or inflammatory response to biomaterials implanted [34]. More recently the use of mathematical models for tissue-engineered angiogenesis that takes into account the interactions between several of the participating cell types into a porous scaffold has provided important insights to more effectively test and evaluate models of interaction [198].

3. CAM as a tool to study vascular development

3.1. Physiological angiogenesis

The ease and accessibility of the CAM is undisputed. Thus, studies that aimed at evaluating the effect of environmental factors in vascular development have taken advantage of this system in a manner that could not be achieved in mammalian systems. Exposure of CAMs to different degrees of CO2 [205] and O2 [206,68], for example, have demonstrated the impact of gases on vascular development. While hypoxia and hyperoxia will be discussed more in detail below, this constitutes a classical example of how the system can be exploited to clarify environmental effects on vascular growth. Similarly, hyperglycemia has been evaluated through a simple process: intravitellus glucose injection [61]. Interestingly, the investigators reported that hyperglycemia decreased angiogenesis as early as day 5 and found a significant increase in apoptosis and pericyte association as early as 2 days post-treatment [61]. These results are consistent with recent findings indicating the negative role of hyperglycemia in angiogenic responses through increase of reactive oxygen species and limitation of VEGFR2 at the cell surface [207].

The CAM has also been used to study localization and levels of molecules in relation to their angiogenic / quiescent status [208,40,209–212]. Thus, it has served as a valuable model system in which to validate expression of relevant vascular molecular pathways. In addition, quail-chicken chimeras have been extensively used to answer questions related to vascular development. For example, the relative plasticity of arterial and venular endothelium has been tested using quail grafts into chicken coelom that acted as hosts. In these experiments, the investigators found that endothelial cells from the grafts of distinct vessels remain plastic even after the acquisition of molecular markers for arteries and veins [213].

Unfortunately, lack of avian-specific reagents (as well as the initially limited genomic information) provided hindrance to a more robust use the CAM in developmental studies of physiological angiogenesis. In this regard, the recent expansion of retroviral, lentiviral and

adenoviral vectors for genomic modification of CAM cells has offered significant advantages to this system [214]. Thus, dominant negative constructs and other tools have been developed to explore the contribution of specific growth factors and signaling cascades in the CAM, in addition to the standard local administration of the growth factor. For example, using manipulation of FGF1 levels, Forough and colleagues showed that neovascularization stimulated by FGF1 could be reduced by selectively targeting AKT signaling [215].

3.2. Hypoxia and hyperoxia

Hypoxia during embryogenesis may induce changes in the development of some physiological regulatory systems, thereby causing permanent phenotypic changes in the e mbryo. Various levels of hypoxia at different time points during embryogenesis were found to affect both anatomical and physiological morphogenesis. Druyan et al. demonstrated that after the 12 h of hypoxic exposure on the CAM, expression of HIF1α, MMP2, VEGF, and VEGFR2 was significantly higher in hypoxic (17% O2) embryos than in controls. In day 6 expression of HIF1α, VEGF, and FGF2 was significantly higher in hypoxic embryos than in controls [216].

Strick et al. conducted the morphometric measurements of chorioallantoic membrane vascularity in chicken eggs that were incubated in various oxygen atmospheres (12, 16, 21, 45, or 70%) beginning on day 7, and vascularity was measured at day 14 [217]. They concluded that hypoxia stimulates and hyperoxia inhibits angiogenesis in the CAM in a dose-related manner. Burton and Palmer showed that hypoxia (17% O2) reduced embryo and CAM growth, but accelerated maturation of the capillary plexus. Hyperoxia (40% O2) had a less marked effect but appeared to retard the final invagination of the plexus, resulting in a thicker air-blood barrier [218].

3.3. Intussusceptive angiogenesis

While most of the growth of the CAM vasculature occurs through sprouting angiogenesis, towards the end of vascular expansion and associated with remodeling processes, intussusceptive microvascular growth also occurs. The process of intussusception is one by which capillaries are generated via the intravascular division of the lumen. This occurs through the growth of thin intraluminar walls (pillars) that proceed to fuse with the opposite side of the vessel. In this manner, the insertion of transcapillary pillars, provides a means to divide vessels further increasing the complexity and number of individual vessels in the vascular plexus. The pillars increase in thickness to include fibroblasts and extracellular matrix increasing in girth and ultimately contribute to separate the vascular segment into two fully independent vessels.

While pillars are discrete structures within the blood stream, relatively isolated from extravascular soluble tissue factors, that are not only identifiable by intravital 2D imaging, but amenable to detailed morphometric analysis. Recent studies have indicated that the number of pillars is the highest between day 8–10 of CAM development and that they are exquisitely responsive to levels of VEGF [219–221]. The pillars are lined with normal-appearing endothelium suggesting a normal responsiveness to intraluminal flow fields [222].

The effect of mechanical forces in shaping pillar geometry, suggested their potential role in initiating pillar formation and potentially explain why they only occur later in CAM development. Most pillars, particularly at vessel bifurcations, demonstrated only small changes in geometry during culture. Lee et al. in their study on physical forces on the CAM concluded that these spatial dynamics reflect a responsiveness of blood vessels to intravascular flow fields and indicate the importance of mechanical forces in shaping both intussusceptive angiogenesis and vessel structure in the microcirculation [223].

3.4. Vasculogenic mimicry

Vasculogenic mimicry (VM) a process by which tumor cells acquire functional features of endothelium and contribute to the formation of the vascular wall has been successfully studied in the CAM [224]. Ribatti et al. showed for the first time the occurrence on VM in the melanoma grafted CAM model after implanting B16-F10 melanoma cells [97]. Since, VM represents an alternative mechanism of tumor vascularization in which tumor cells actively participate in the formation of blood vessels. Its demonstration in the CAM provides an important validation step that can be further explored.

3. Physical forces in the CAM

Hemodynamic forces, including vascular circumferential tension and shear stress, have been predicted to influence angiogenesis. Recently, Branum and colleagues tested this hypothesis directly by evaluating the effect of pharmacological induction of acute and chronic bradycardia in chicken embryos. Contrary to predictions, the investigators found that vascular density of smaller vessels was reduced, but larger vessels were not significantly affected [225].

In terms of vascular remodeling, physical forces are also known to contribute to the progression of the uniformed primary plexus into a hierarchic vascular tree. It is also known that arterialization of veins can occur when subjected to high shear stress forces. For example saphenous veins used in coronary bypass grafts to substitute occluded arteries show signs or arterialization. Using the CAM, investigators have explored whether molecular identity of arteries and veins is also governed by flow. In an elegant series of experiments le Noble and colleagues showed that arterial-venous differentiation is in fact a flow driven highly dynamic process that relies on the plasticity of the endothelium [226].

In addition to genetic and biochemical signaling, the expansion and remodeling of a vascular supply is controlled by microenvironmental signals such as mechanical forces conveye d by extracellular matrix (ECM) and by flow. Although capillary development is driven by angiogenic mitogens, cell sensitivity to them might be modulated by a complex set of physical interactions between cells and ECM that alter the cellular cytoskeleton [227]. Changes in capillary cell shape and function can be produced by altering ECM elasticity or topography, as these provide mechanical stresses that impact traction forces [228]. Mechanical forces may also stimulate vascular remodeling and capillary growth *in vivo* [229,230]. Kilarski et al. found that tissue tension is generated by activated fibroblasts or myofibroblasts during wound contraction followed by the induction of new vasculature. These mechanical forces pulled vessels from the preexisting vascular bed with functional

circulation that expanded as an integral part of the growing granulation tissue through vessel enlargement and elongation [230].

The mechanical forces associated with blood flow include wall shear stress (the frictional force tangential to the vessel wall) and circumferential strain (a blood pressure related force perpendicular to the direction of flow); wall shear stress being the dominant mechanical force in the smooth and continuous flow of the peripheral CAM microcirculation [222]. Although wall shear stress cannot be directly measured, numerical simulations enable not only the calculation of wall shear stress but the mapping of these mechanical forces to the vessel wall. The spatial relationships revealed by these maps provide important insights into the role of mechanical forces in shaping the structure of vessels and alters their responses during pathological conditions.

5. Closing remarks

Despite enormous volume of information generated by *in vitro* tests, *in vivo* experimentation offers a stronger reliable value when assessing angiogenic responses. *In vivo* assays usually require special skills and ethical committee approvals, thereby limiting the number of tests that can readily be performed. As presented in this review, the CAM model has been used effectively by several disciplines including biology, medicine and bioengineering to determine vascular responses and to explore questions related to blood vessel and lymphatic morphogenesis and physiology. Numerous and continuous improvements in imaging and quantification continue to offer strengths to the model. Furthermore, while not mammalian, the CAM offers a valuable intermediate step that is both cost and time-efficient. Finally, considering the pressures with minimizing the use of animal models and following the “3R” rule (*Replacement*, *Refinement and Reduction*) the CAM provides an excellent intermediary step prior to pre-clinical evaluation.

Acknowledgments

The authors acknowledge Dr. Valentin Djonov for delivery of the unpublished scanning electron microscopy image (Figure 10c) and Dr. Steven Menzler for the images shown in Figure 10a,d.

Abbreviations

AA	anti-angiogenic
AC	anti-cancer
ALA	aminolevulinic acid
AM	anti-microbial
AMD	age-related macular degeneration
BrdU	bromodeoxyuridine
CAM	chicken chorioallantoic membrane
CNV	subfoveal choroidal neovascularization

DDS	drug delivery systems
DPPC	dipalmitoylphosphatidylcholine
ECs	endothelial cells
ECM	extracellular matrix
GF	growth factor
HGF	hepatocyte growth factor
LC	Langerhans cells
LF	lipid factor
MR	microbeam radiation
PCV	polypoidal choroidal vasculopathy
PDD	photodynamic diagnosis
PEG	polyethylene glycol
PLGA	poly(lactide-co-glycolide)
PpIX	protoporphyrin IX
Prox1	prospero homeobox protein 1
PS	photosensitizer
SMA	smooth muscle actin
VDA	vascular disrupting agents
VM	vasculogenic mimicry
YSM	yolk sac membrane

References

1. Rous P, Murphy JB. Tumor implantations in the developing embryo. J Am Med Assoc. 1911; 56:741–741.
2. Murphy JB. Transplantability of malignant tumors to embryos of a foreign species. J Am Med Assoc. 1912; 59:874.
3. Goodpasture EW, Woodruff AM, Buddingh GJ. The Cultivation of Vaccine and Other Viruses in the Chorioallantoic Membrane of Chick Embryos. Science. 1931; 74(1919):371–372. [PubMed: 17810781]
4. Morrow G, Syverton JT, Stiles WW, Berry GP. The Growth of Leptospira Icterohemorrhagiae on the Chorioallantoic Membrane of the Chick Embryo. Science. 1938; 88(2286):384–385. [PubMed: 17746419]
5. Moore M. The Chorioallantoic Membrane of Chick Embryos and Its Response to Inoculation with Some Mycobacteria. Am J Pathol. 1942; 18(5):827–847. [PubMed: 19970658]
6. Ribatti D, Vacca A, Roncali L, Dammacco F. The chick embryo chorioallantoic membrane as a model for in vivo research on anti-angiogenesis. Curr Pharm Biotechnol. 2000; 1(1):73–82. [PubMed: 11467363]
7. Ribatti D. Chicken chorioallantoic membrane angiogenesis model. Methods Mol Biol. 2012; 843:47–57. [PubMed: 22222520]

8. Auerbach R, Kubai L, Knighton D, Folkman J. A simple procedure for the long-term cultivation of chicken embryos. Dev Biol. 1974; 41(2):391–394. [PubMed: 4452416]
9. Nguyen M, Shing Y, Folkman J. Quantitation of angiogenesis and antiangiogenesis in the chick embryo chorioallantoic membrane. Microvasc Res. 1994; 47(1):31–40. [PubMed: 7517489]
10. Vazquez F, Hastings G, Ortega MA, Lane TF, Oikemus S, Lombardo M, Iruela-Arispe ML. METH-1, a human ortholog of ADAMTS-1, and METH-2 are members of a new family of proteins with angio-inhibitory activity. J Biol Chem. 1999; 274(33):23349–23357. [PubMed: 10438512]
11. Hamburger V, Hamilton H. A series of normal stages in the development of the chick embryo. J Morphol. 1951; 88:49–92. [PubMed: 24539719]
12. Papoutsi M, Tomarev SI, Eichmann A, Prols F, Christ B, Wilting J. Endogenous origin of the lymphatics in the avian chorioallantoic membrane. Dev Dynam. 2001; 222(2):238–251.
13. Ribatti D. The Chick Embryo Chorioallantoic Membrane in the Study of Angiogenesis and Metastasis. Springer Science & Business Media. 2010
14. Dohle DS, Pasa SD, Gustmann S, Laub M, Wissler JH, Jennissen HP, Dunker N. Chick ex ovo culture and ex ovo CAM assay: how it really works. JoVE. 2009; (33)10.3791/1620
15. Burnet FM. A virus disease of the canary of the fowl-pox group. J Pathol Bacteriol. 1933; 37:107–122.
16. Dagg CP, Karnofsky DA, Roddy J. Growth of transplantable human tumors in the chick embryo and hatched chick. Cancer Res. 1956; 16(7):589–594. [PubMed: 13356282]
17. Zwilling E. A modified chorioallantoic grafting procedure. Transplant Bull. 1959; 6(1):115–116. [PubMed: 13635839]
18. Nowak-Sliwinska P, van Beijnum JR, van Berkel M, van den Bergh H, Griffioen AW. Vascular regrowth following photodynamic therapy in the chicken embryo chorioallantoic membrane. Angiogenesis. 2010; 13(4):281–292. [PubMed: 20842454]
19. Nowak-Sliwinska P, Weiss A, Beijnum JR, Wong TJ, Ballini JP, Lovisa B, van den Bergh H, Griffioen AW. Angiostatic kinase inhibitors to sustain photodynamic angio-occlusion. J Cell Mol Med. 2012; 16(7):1553–1562. [PubMed: 21880113]
20. Lange N, Ballini JP, Wagnieres G, van den Bergh H. A new drug-screening procedure for photosensitizing agents used in photodynamic therapy for CNV. Invest Ophthalmol Vis Sci. 2001; 42(1):38–46. [PubMed: 11133846]
21. Abe C, Uto Y, Nakae T, Shinmoto Y, Sano K, Nakata H, Teraoka M, Endo Y, Maezawa H, Masunaga S, Nakata E, Hori H. Evaluation of the in vivo radiosensitizing activity of etanidazole using tumor-bearing chick embryo. J Radiat Res. 2011; 52(2):208–214. [PubMed: 21436611]
22. Kardamakis D, Hadjimichael C, Ginopoulos P, Papaioannou S. Effects of paclitaxel in combination with ionizing radiation on angiogenesis in the chick embryo chorioallantoic membrane. A radiobiological study. Strahlenther Onkol. 2004; 180(3):152–156. [PubMed: 14991203]
23. Wilson SM, Chambers AF. Experimental metastasis assays in the chick embryo. Curr Prot Cell BIOL. 2004:16. Chapter 19: Unit 19.
24. Borges J, Tegtmeier FT, Padron NT, Mueller MC, Lang EM, Stark GB. Chorioallantoic membrane angiogenesis model for tissue engineering: a new twist on a classic model. Tissue Eng. 2003; 9(3): 441–450. [PubMed: 12857412]
25. Ponce ML, Kleinman HK. The Chick Chorioallantoic Membrane as an In Vivo Angiogenesis Model. Curr Protoc Cell Biol. 2003; 191:5. 1–6. [PubMed: 18228425]
26. Ribatti D, Nico B, Vacca A, Presta M. The gelatin sponge-chorioallantoic membrane assay. Nat Protoc. 2006; 1(1):85–91. [PubMed: 17406216]
27. Ausprunk DH, Knighton DR, Folkman J. Differentiation of vascular endothelium in the chick chorioallantois: a structural and autoradiographic study. Dev Biol. 1974; 38(2):237–248. [PubMed: 4831108]
28. Kucera P, Burnand MB. Routine teratogenicity test that uses chick embryos in vitro. Teratogen Carcin Mut. 1987; 7(5):427–447.
29. Samkoe KS, Clancy AA, Karotki A, Wilson BC, Cramb DT. Complete blood vessel occlusion in the chick chorioallantoic membrane using two-photon excitation photodynamic therapy:

implications for treatment of wet age-related macular degeneration. J Biomed Opt. 2007; 12(3): 034025. [PubMed: 17614733]

30. Deryugina EI, Quigley JP. Chapter 2. Chick embryo chorioallantoic membrane models to quantify angiogenesis induced by inflammatory and tumor cells or purified effector molecules. Meth Enzymol. 2008; 444:21–41. [PubMed: 19007659]
31. Lei Y, Rahim M, Ng Q, Segura T. Hyaluronic acid and fibrin hydrogels with concentrated DNA/PEI polyplexes for local gene delivery. J Control Release. 2011; 153(3):255–261. [PubMed: 21295089]
32. Weiss A, van Beijnum JR, Bonvin D, Jichlinski P, Dyson PJ, Griffioen AW, Nowak-Sliwinska P. Low-dose angiostatic tyrosine kinase inhibitors improve photodynamic therapy for cancer: lack of vascular normalization. J Cell Mol Med. 2014; 18(3):480–491. [PubMed: 24450440]
33. Grummer R. Animal models in endometriosis research. Hum Reprod Update. 2006; 12(5):641–649. [PubMed: 16775193]
34. Valdes TI, Kreutzer D, Moussy F. The chick chorioallantoic membrane as a novel in vivo model for the testing of biomaterials. J Biomed Mater Res. 2002; 62(2):273–282. [PubMed: 12209948]
35. Valdes TI, Klueh U, Kreutzer D, Moussy F. Ex ova chick chorioallantoic membrane as a novel in vivo model for testing biosensors. J Biomed Mater Res Part A. 2003; 67(1):215–223.
36. Ribatti D, Nico B, Vacca A, Roncali L, Burri PH, Djonov V. Chorioallantoic membrane capillary bed: a useful target for studying angiogenesis and anti-angiogenesis in vivo. Anat Rec. 2001; 264(4):317–324. [PubMed: 11745087]
37. Reuwer AQ, Nowak-Sliwinska P, Mans LA, van der Loos CM, von der Thüsen JH, Twickler MT, Spek CA, Goffin V, Griffioen AW, Borensztajn KS. Functional consequences of prolactin signaling in endothelial cells: a potential link with angiogenesis in pathophysiology? J Cell Mol Med. 2012; 16(9):2035–2048. [PubMed: 22128761]
38. Gagliardi A, Collins DC. Inhibition of angiogenesis by antiestrogens. Cancer Res. 1993; 53(3): 533–535. [PubMed: 7678775]
39. Adar Y, Stark M, Bram EE, Nowak-Sliwinska P, van den Bergh H, Szewczyk G, Sarna T, Skladanowski A, Griffioen AW, Assaraf YG. Imidazoacridinone-dependent lysosomal photodestruction: a pharmacological Trojan horse approach to eradicate multidrug-resistant cancers. Cell Death Dis. 2012; 3:e293. [PubMed: 22476101]
40. Pipili-Synetos E, Kritikou S, Papadimitriou E, Athanassiadou A, Flordellis C, Maragoudakis ME. Nitric oxide synthase expression, enzyme activity and NO production during angiogenesis in the chick chorioallantoic membrane. Brit J Pharmacol. 2000; 129(1):207–213. [PubMed: 10694222]
41. Clavel CM, Paunescu E, Nowak-Sliwinska P, Griffioen AW, Scopelliti R, Dyson PJ. Discovery of a Highly Tumor-Selective Organometallic Ruthenium(II)-Arene Complex. J Med Chem. 2014; 57(8):3546–3558. [PubMed: 24669938]
42. Nowak-Sliwinska P, van Beijnum JR, Casini A, Nazarov AA, Wagnieres G, van den Bergh H, Dyson PJ, Griffioen AW. Organometallic Ruthenium(II) Arene Compounds with Antiangiogenic Activity. J MEd Chem. 2011; 54(11):3895–3902. [PubMed: 21534534]
43. Nazarov AA, Baquie M, Nowak-Sliwinska P, Zava O, van Beijnum JR, Groessl M, Chisholm DM, Ahmadi Z, McIndoe JS, Griffioen AW, van den Bergh H, Dyson PJ. Synthesis and characterization of a new class of anti-angiogenic agents based on ruthenium clusters. Sci Rep. 2013; 3:1485. [PubMed: 23508096]
44. Hu GF. Neomycin inhibits angiogenin-induced angiogenesis. Proc Nat Acad Sci. 1998; 95(17): 9791–9795. [PubMed: 9707554]
45. Nowak-Sliwinska P, Storto M, Cataudella T, Ballini JP, Gatz R, Giorgio M, van den Bergh H, Plyte S, Wagnières G. Angiogenesis inhibition by the maleimide-based small molecule GNX-686. Microvasc Res. 2012; 83:105–110. [PubMed: 22056402]
46. van Beijnum JR, Nowak-Sliwinska P, van den Boezem E, Hautvast P, Buurman WA, Griffioen AW. Tumor angiogenesis is enforced by autocrine regulation of high-mobility group box 1. Oncogene. 2013; 17(32):363–374. [PubMed: 22391561]
47. Form DM, Auerbach R. PGE2 and angiogenesis. Proc Soc Exp Biol Med. 1983; 172(2):214–218. [PubMed: 6572402]

48. Chen Z, Milner TE, Srinivas S, Wang X, Malekafzali A, van Gemert MJ, Nelson JS. Noninvasive imaging of in vivo blood flow velocity using optical Doppler tomography. Opt Lett. 1997; 22(14): 1119–1121. [PubMed: 18185770]
49. Tay SL, Heng PW, Chan LW. The CAM-LDPI method: a novel platform for the assessment of drug absorption. J Pharm Pharmacol. 2012; 64(4):517–529. [PubMed: 22420658]
50. Liu X, Zhang K, Huang Y, Kang JU. Spectroscopic-speckle variance OCT for microvasculature detection and analysis. Biomed Opt Express. 2011; 2(11):2995–3009. [PubMed: 22076262]
51. Debefve E, Pegaz B, van den Bergh H, Wagnieres G, Lange N, Ballini JP. Video monitoring of neovessel occlusion induced by photodynamic therapy with verteporfin (Visudyne), in the CAM model. Angiogenesis. 2008; 11(3):235–243. [PubMed: 18324477]
52. Chambers AF, Schmidt EE, MacDonald IC, Morris VL, Groom AC. Early steps in hematogenous metastasis of B16F1 melanoma cells in chick embryos studied by high-resolution intravital videomicroscopy. J Natl Cancer Inst. 1992; 84(10):797–803. [PubMed: 1573668]
53. Hlushchuk R, Ehrbar M, Reichmuth P, Heinimann N, Styp-Rekowska B, Escher R, Baum O, Lienemann P, Makanya A, Keshet E, Djonov V. Decrease in VEGF expression induces intussusceptive vascular pruning. Arterioscler Thromb Vasc Biol. 2011; 31(12):2836–2844. [PubMed: 21921259]
54. Chesnick IE, Fowler CB, Mason JT, Potter K. Novel mineral contrast agent for magnetic resonance studies of bone implants grown on a chick chorioallantoic membrane. Magn Reson Im. 2011; 29(9):1244–1254.
55. Warnock G, Turtoi A, Blomme A, Bretin F, Bahri MA, Lemaire C, Libert LC, Seret AE, Luxen A, Castronovo V, Plenevaux AR. In vivo PET/CT in a human glioblastoma chicken chorioallantoic membrane model: a new tool for oncology and radiotracer development. J Nucl Med. 2013; 54(10):1782–1788. [PubMed: 23970367]
56. Miller WJ, Kayton ML, Patton A, O'Connor S, He M, Vu H, Baibakov G, Lorang D, Knezevic V, Kohn E, Alexander HR, Stirling D, Payvandi F, Muller GW, Libutti SK. A novel technique for quantifying changes in vascular density, endothelial cell proliferation and protein expression in response to modulators of angiogenesis using the chick chorioallantoic membrane (CAM) assay. J Transl Med. 2004; 2(1):4. [PubMed: 14754458]
57. Zeng L, Da X, Gu H, Yang D, Yang S, Xiang L. High antinoise photoacoustic tomography based on a modified filtered backprojection algorithm with combination wavelet. Med Phys. 2007; 34(2): 556–563. [PubMed: 17388173]
58. Faez T, Skachkov I, Versluis M, Kooiman K, de Jong N. In vivo characterization of ultrasound contrast agents: microbubble spectroscopy in a chicken embryo. Ultrasound Med Biol. 2012; 38(9):1608–1617. [PubMed: 22766113]
59. Ford TN, Lim D, Mertz J. Fast optically sectioned fluorescence HiLo endomicroscopy. J Biomed Opt. 2012; 17(2):021105. [PubMed: 22463023]
60. Kirchner LM, Schmidt SP, Gruber BS. Quantitation of angiogenesis in the chick chorioallantoic membrane model using fractal analysis. Microvasc Res. 1996; 51(1):2–14. [PubMed: 8812748]
61. Larger E, Marre M, Corvol P, Gasc JM. Hyperglycemia-induced defects in angiogenesis in the chicken chorioallantoic membrane model. Diabetes. 2004; 53(3):752–761. [PubMed: 14988261]
62. Blacher S, Davy L, Hlushchuk R, Larger E, Lamande N, Burri P, Corvol P, Djonov V, Foidart JM, Noel A. Quantification of angiogenesis in the chicken chorioallantoic membrane (CAM). Image Anal Stereol. 2005; 24:169–180.
63. Doukas CN, Maglogiannis I, Chatziioannou AA. Computer-supported angiogenesis quantification using image analysis and statistical averaging. IEEE Trans Inf Technol Biomed. 2008; 12(5):650–657. [PubMed: 18779080]
64. Nowak-Sliwinska P, Ballini J-P, Wagnières G, van den Bergh H. Processing of fluorescence angiograms for the quantification of vascular effects induced by anti-angiogenic agents in the CAM model. Microvasc Res. 2010; 79(1):21–28. [PubMed: 19857502]
65. Parsons-Wingerter P, Lwai B, Yang MC, Elliott KE, Milaninia A, Redlitz A, Clark JI, Sage EH. A novel assay of angiogenesis in the quail chorioallantoic membrane: stimulation by bFGF and inhibition by angiostatin according to fractal dimension and grid intersection. Microvasc Res. 1998; 55(3):201–214. [PubMed: 9657920]

66. Doukas CN, Maglogiannis I, Chatziioannou A, Papapetropoulos A. Automated angiogenesis quantification through advanced image processing techniques. Conf Proc IEEE Eng Med Biol Soc. 2006; 1:2345–2348. [PubMed: 17946107]

67. Pyriochou A, Tsigkos S, Vassilakopoulos T, Cottin T, Zhou Z, Gourzoulidou E, Roussos C, Waldmann H, Giannis A, Papapetropoulos A. Anti-angiogenic properties of a sulindac analogue. Brit J Pharmacol. 2007; 152(8):1207–1214. [PubMed: 17965739]

68. Strick DM, Waycaster RL, Montani JP, Gay WJ, Adair TH. Morphometric measurements of chorioallantoic membrane vascularity: effects of hypoxia and hyperoxia. Am J Physiol. 1991; 260(4 Pt 2):H1385–1389. [PubMed: 2012235]

69. Vickerman MB, Keith PA, McKay TL, Gedeon DJ, Watanabe M, Montano M, Karunamuni G, Kaiser PK, Sears JE, Ebrahem Q, Ribita D, Hylton AG, Parsons-Wingerter P. VESGEN 2D: automated, user-interactive software for quantification and mapping of angiogenic and lymphangiogenic trees and networks. Anat Rec (Hoboken, NJ: 2007). 2009; 292(3):320–332.

70. Javerzat S, Franco M, Herbert J, Platonova N, Peille AL, Pantesco V, De Vos J, Assou S, Bicknell R, Bikfalvi A, Hagedorn M. Correlating global gene regulation to angiogenesis in the developing chick extra-embryonic vascular system. PLoS One. 2009; 4(11):e7856. [PubMed: 19924294]

71. Ausprunk DH, Knighton DR, Folkman J. Vascularization of normal and neoplastic tissues grafted to the chick chorioallantois. Role of host and preexisting graft blood vessels. Am J Pathol. 1975; 79(3):597–618. [PubMed: 1094838]

72. Barrie R, Woltering EA, Hajarizadeh H, Mueller C, Ure T, Fletcher WS. Inhibition of angiogenesis by somatostatin and somatostatin-like compounds is structurally dependent. J Surg Res. 1993; 55(4):446–450. [PubMed: 7692142]

73. Deryugina EI, Quigley JP. Chick embryo chorioallantoic membrane model systems to study and visualize human tumor cell metastasis. Histochem Cell Biol. 2008; 130(6):1119–1130. [PubMed: 19005674]

74. Tay SL, Heng PW, Chan LW. The chick chorioallantoic membrane imaging method as a platform to evaluate vasoactivity and assess irritancy of compounds. J Pharm Pharmacol. 2012; 64(8):1128–1137. [PubMed: 22775216]

75. DeFouw DO, Rizzo VJ, Steinfeld R, Feinberg RN. Mapping of the microcirculation in the chick chorioallantoic membrane during normal angiogenesis. Microvasc Res. 1989; 38(2):136–147. [PubMed: 2477666]

76. Dimitropoulou C, Malkusch W, Fait E, Maragoudakis ME, Konerding MA. The vascular architecture of the chick chorioallantoic membrane: sequential quantitative evaluation using corrosion casting. Angiogenesis. 1998; 2(3):255–263. [PubMed: 14517465]

77. Burton GJ, Palmer ME. The chorioallantoic capillary plexus of the chicken egg: a microvascular corrosion casting study. Scanning Microscopy. 1989; 3(2):549–557. [PubMed: 2814401]

78. Seidlitz E, Korbie D, Marien L, Richardson M, Singh G. Quantification of anti-angiogenesis using the capillaries of the chick chorioallantoic membrane demonstrates that the effect of human angiostatin is age-dependent. Microvasc Res. 2004; 67(2):105–116. [PubMed: 15020201]

79. Parsons-Wingerter P, McKay TL, Leontiev D, Vickerman MB, Condrich TK, Dicorleto PE. Lymphangiogenesis by blind-ended vessel sprouting is concurrent with hemangiogenesis by vascular splitting. Anat Rec Part A, Discoveries in molecular, cellular, and evolutionary biology. 2006; 288(3):233–247.

80. Cimpean AM, Seclaman E, Ceausu R, Gaje P, Feflea S, Anghel A, Raica M, Ribatti D. VEGF-A/HGF induce Prox-1 expression in the chick embryo chorioallantoic membrane lymphatic vasculature. Clin Exp Med. 2010; 10(3):169–172. [PubMed: 20033752]

81. Oh SJ, Jeltsch MM, Birkenhager R, McCarthy JE, Weich HA, Christ B, Alitalo K, Wilting J. VEGF and VEGF-C: specific induction of angiogenesis and lymphangiogenesis in the differentiated avian chorioallantoic membrane. Develop Biol. 1997; 188(1):96–109. [PubMed: 9245515]

82. Oliver G, Detmar M. The rediscovery of the lymphatic system: old and new insights into the development and biological function of the lymphatic vasculature. Gene Dev. 2002; 16(7):773–783. [PubMed: 11937485]

83. Papoutsi M, Sleeman JP, Wilting J. Interaction of rat tumor cells with blood vessels and lymphatics of the avian chorioallantoic membrane. Microsc Res Tech. 2001; 55(2):100–107. [PubMed: 11596155]
84. Holzmann P, Niculescu-Morzsa E, Zwickl H, Halbwirth F, Pichler M, Matzner M, Gottsauner-Wolf F, Nehrer S. Investigation of bone allografts representing different steps of the bone bank procedure using the CAM-model. Altex. 2010; 27(2):97–103. [PubMed: 20686742]
85. Pink DB, Schulte W, Parseghian MH, Zijlstra A, Lewis JD. Real-time visualization and quantitation of vascular permeability in vivo: implications for drug delivery. PLoS One. 2012; 7(3):e33760. [PubMed: 22479438]
86. Debefve E, Pegaz B, Ballini JP, Konan YN, van den Bergh H. Combination therapy using aspirin-enhanced photodynamic selective drug delivery. Vasc Pharmacol. 2007; 46(3):171–180.
87. Rizzo V, DeFouw DO. Microvascular permselectivity in the chick chorioallantoic membrane during endothelial cell senescence. Int J Microcirc Clin Exp. 1997; 17(2):75–79. [PubMed: 9253684]
88. Rizzo V, Steinfeld R, Kyriakides C, DeFouw DO. The microvascular unit of the 6-day chick chorioallantoic membrane: a fluorescent confocal microscopic and ultrastructural morphometric analysis of endothelial permselectivity. Microvasc Res. 1993; 46(3):320–332. [PubMed: 8121316]
89. van der Horst EH, Frank BT, Chinn L, Coxon A, Li S, Polesso F, Slavin A, Ruefli-Brasse A, Wesche H. The growth factor Midkine antagonizes VEGF signaling in vitro and in vivo. Neoplasia. 2008; 10(4):340–347. [PubMed: 18392135]
90. Flamme I, von Reutern M, Drexler HC, Syed-Ali S, Risau W. Overexpression of vascular endothelial growth factor in the avian embryo induces hypervascularization and increased vascular permeability without alterations of embryonic pattern formation. Dev Biol. 1995; 171(2):399–414. [PubMed: 7556923]
91. Stieger SM, Caskey CF, Adamson RH, Qin S, Curry FR, Wisner ER, Ferrara KW. Enhancement of vascular permeability with low-frequency contrast-enhanced ultrasound in the chorioallantoic membrane model. Radiology. 2007; 243(1):112–121. [PubMed: 17392250]
92. Murphy JB. Transplantability of Tissues to the Embryo of Foreign Species: Its Bearing on Questions of Tissue Specificity and Tumor Immunity. J Exp Med. 1913; 17(4):482–493. [PubMed: 19867659]
93. Subauste MC, Kupriyanova TA, Conn EM, Ardi VC, Quigley JP, Deryugina EI. Evaluation of metastatic and angiogenic potentials of human colon carcinoma cells in chick embryo model systems. Clin Exp Metastas. 2009; 26(8):1033–1047.
94. Sys GM, Lapeire L, Stevens N, Favoreel H, Forsyth R, Bracke M, De Wever O. The in ovo CAM-assay as a xenograft model for sarcoma. JoVE. 2013; (77):e50522. [PubMed: 23892612]
95. Fergelot P, Bernhard JC, Soulet F, Kilarski WW, Leon C, Courtois N, Deminiere C, Herbert JM, Antczak P, Falciani F, Rioux-Leclercq N, Patard JJ, Ferriere JM, Ravaud A, Hagedorn M, Bikfalvi A. The experimental renal cell carcinoma model in the chick embryo. Angiogenesis. 2013; 16(1): 181–194. [PubMed: 23076651]
96. Balke M, Neumann A, Kersting C, Agelopoulos K, Gebert C, Gosheger G, Buerger H, Hagedorn M. Morphologic characterization of osteosarcoma growth on the chick chorioallantoic membrane. BMC. 2010; 3:58.
97. Ribatti D, Nico B, Cimpean AM, Raica M, Crivellato E, Ruggieri S, Vacca A. B16-F10 melanoma cells contribute to the new formation of blood vessels in the chick embryo chorioallantoic membrane through vasculogenic mimicry. Clin Exp Med. 2013; 13(2):143–147. [PubMed: 22527563]
98. Ribatti D, De Falco G, Nico B, Ria R, Crivellato E, Vacca A. In vivo time-course of the angiogenic response induced by multiple myeloma plasma cells in the chick embryo chorioallantoic membrane. J Anat. 2003; 203(3):323–328. [PubMed: 14529049]
99. Gronau S, Thess B, Riechelmann H, Fischer Y, Schmitt A, Schmitt M. An autologous system for culturing head and neck squamous cell carcinomas for the assessment of cellular therapies on the chorioallantois membrane. Eur Arch Otorhinolaryngol. 2006; 263(4):308–312. [PubMed: 16252122]

100. Auerbach R, Kubai L, Sidky Y. Angiogenesis induction by tumors, embryonic tissues, and lymphocytes. Cancer Res. 1976; 36(9 PT 2):3435–3440. [PubMed: 975113]

101. Klagsbrun M, Knighton D, Folkman J. Tumor angiogenesis activity in cells grown in tissue culture. Cancer Res. 1976; 36(1):110–114. [PubMed: 1247990]

102. Marzullo A, Vacca A, Roncali L, Pollice L, Ribatti D. Angiogenesis in hepatocellular carcinoma: an experimental study in the chick embryo chorioallantoic membrane. Int J Oncol. 1998; 13(1): 17–21. [PubMed: 9625798]

103. Brooks PC, Montgomery AM, Rosenfeld M, Reisfeld RA, Hu T, Klier G, Cheresh DA. Integrin alpha v beta 3 antagonists promote tumor regression by inducing apoptosis of angiogenic blood vessels. Cell. 1994; 79(7):1157–1164. [PubMed: 7528107]

104. Kunzi-Rapp K, Kaskel P, Steiner R, Peter RU, Krahn G. Increased blood levels of human S100 in melanoma chick embryo xenografts' circulation. Pigment Cell Res. 2001; 14(1):9–13. [PubMed: 11277496]

105. Ismail MS, Torsten U, Dressler C, Diederichs JE, Huske S, Weitzel H, Berlien HP. Photodynamic therapy of malignant ovarian tumors cultivated on CAM. Laser Med Sci. 1999; 14:91–96.

106. Isachenko V, Mallmann P, Petrunkina AM, Rahimi G, Nawroth F, Hancke K, Felberbaum R, Genze F, Damjanoski I, Isachenko E. Comparison of in vitro- and chorioallantoic membrane (CAM)-culture systems for cryopreserved medulla-contained human ovarian tissue. PLoS One. 2012; 7(3):e32549. [PubMed: 22479331]

107. Cimpean AM, Ribatti D, Raica M. The chick embryo chorioallantoic membrane as a model to study tumor metastasis. Angiogenesis. 2008; 11(4):311–319. [PubMed: 18780151]

108. Isachenko V, Orth I, Isachenko E, Mallmann P, Peters D, Schmidt T, Morgenstern B, Foth D, Hanstein B, Rahimi G. Viability of human ovarian tissue confirmed 5 years after freezing with spontaneous ice-formation by autografting and chorio-allantoic membrane culture. Cryobiology. 2013; 66(3):233–238. [PubMed: 23454031]

109. Isachenko V, Isachenko E, Mallmann P, Rahimi G. Increasing follicular and stromal cell proliferation in cryopreserved human ovarian tissue after long-term precooling prior to freezing: in vitro versus chorioallantoic membrane (CAM) xenotransplantation. Cell Transplantat. 2013; 22(11):2053–2061.

110. Deryugina EI, Zijlstra A, Partridge JJ, Kupriyanova TA, Madsen MA, Papagiannakopoulos T, Quigley JP. Unexpected effect of matrix metalloproteinase down-regulation on vascular intravasation and metastasis of human fibrosarcoma cells selected in vivo for high rates of dissemination. Cancer Res. 2005; 65(23):10959–10969. [PubMed: 16322244]

111. Lokman NA, Elder AS, Ricciardelli C, Oehler MK. Chick Chorioallantoic Membrane (CAM) Assay as an In Vivo Model to Study the Effect of Newly Identified Molecules on Ovarian Cancer Invasion and Metastasis. Int J Mol Sci. 2012; 13(8):9959–9970. [PubMed: 22949841]

112. Becker J, Covelo-Fernandez A, von Bonin F, Kube D, Wilting J. Specific tumor-stroma interactions of EBV-positive Burkitt's lymphoma cells in the chick chorioallantoic membrane. Vascular Cell. 2012; 4(1):3. [PubMed: 22404859]

113. Lugassy C, Kleinman HK, Vernon SE, Welch DR, Barnhill RL. C16 laminin peptide increases angiotropic extravascular migration of human melanoma cells in a shell-less chick chorioallantoic membrane assay. Brit J Dermatol. 2007; 157(4):780–782. [PubMed: 17711523]

114. van den Bergh, H.; Ballini, JP. Photodynamic therapy: basic principle. In: FFaK, S., editor. Lasers in Ophthalmology - Basic, diagnostic and Surgical Aspects. Kugler Publications; The Hague: 2003. p. 183-195.

115. Weiss A, van den Bergh H, Griffioen AW, Nowak-Sliwinska P. Angiogenesis inhibition for the improvement of photodynamic therapy: the revival of a promising idea. BBA Rev Cancer. 2012; 1826(1):53–70.

116. Lim SH, Nowak-Sliwinska P, Kamarulzaman FA, van den Bergh H, Wagnieres G, Lee HB. The neovessel occlusion efficacy of 15-hydroxypurpurin-7-lactone dimethyl ester induced with photodynamic therapy. Photochem Photobiol. 2010; 86(2):397–402. [PubMed: 20074086]

117. Pegaz B, Debefve E, Ballini JP, Wagnieres G, Spaniol S, Albrecht V, Scheglmann DV, Nifantiev NE, van den Bergh H, Konan-Kouakou YN. Photothrombic activity of m-THPC-loaded

liposomal formulations: pre-clinical assessment on chick chorioallantoic membrane model. Eur J Pharm Sci. 2006; 28(1–2):134–140. [PubMed: 16504490]

118. Pegaz B, Debefve E, Borle F, Ballini JP, Wagnieres G, Spaniol S, Albrecht V, Scheglmann D, Nifantiev NE, van den Bergh H, Konan YN. Preclinical evaluation of a novel water-soluble chlorin E6 derivative (BLC 1010) as photosensitizer for the closure of the neovessels. Photochem Photobiol. 2005; 81(6):1505–1510. [PubMed: 15960590]
119. Olivo M, Chin W. Perylenequinones in photodynamic therapy: cellular versus vascular response. J Environ Pathol Toxicol Oncol. 2006; 25(1–2):223–237. [PubMed: 16566720]
120. Hammer-Wilson MJ, Cao D, Kimel S, Berns MW. Photodynamic parameters in the chick chorioallantoic membrane (CAM) bioassay for photosensitizers administered intraperitoneally (IP) into the chick embryo. Photochem Photobiol Sci. 2002; 1(9):721–728. [PubMed: 12665312]
121. Piffaretti F, Novello AM, Kumar RS, Forte E, Paulou C, Nowak-Sliwinska P, van den Bergh H, Wagnieres G. Real-time, in vivo measurement of tissular pO2 through the delayed fluorescence of endogenous protoporphyrin IX during photodynamic therapy. J Biomed Opt. 2012; 17(11): 115007. [PubMed: 23214178]
122. Pegaz B, Debefve E, Borle F, Ballini JP, van den Bergh H, Kouakou-Konan YN. Encapsulation of porphyrins and chlorins in biodegradable nanoparticles: the effect of dye lipophilicity on the extravasation and the photothrombic activity. A comparative study. J Photochem Photobiol B. 2005; 80(1):19–27. [PubMed: 15963434]
123. Gottfried V, Davidi R, Averguj C, Kimel S. In vivo damage to chorioallantoic membrane blood vessels by porphycene-induced photodynamic therapy. J Photochem Photobiol B. 1995; 30(2–3): 115–121. [PubMed: 8558365]
124. Saw CL, Olivo M, Soo KC, Heng PW. Delivery of hypericin for photodynamic applications. Cancer Lett. 2006; 241(1):23–30. [PubMed: 16303248]
125. Pastorino F, Brignole C, Di Paolo D, Nico B, Pezzolo A, Marimpietri D, Pagnan G, Piccardi F, Cilli M, Longhi R, Ribatti D, Corti A, Allen TM, Ponzoni M. Targeting liposomal chemotherapy via both tumor cell-specific and tumor vasculature-specific ligands potentiates therapeutic efficacy. Cancer Res. 2006; 66(20):10073–10082. [PubMed: 17047071]
126. Knoll A, Schmidt S, Chapman M, Wiley D, Bulgrin J, Blank J, Kirchner L. A comparison of two controlled-release delivery systems for the delivery of amiloride to control angiogenesis. Microvasc Res. 1999; 58(1):1–9. [PubMed: 10388598]
127. Wacker BK, Scott EA, Kaneda MM, Alford SK, Elbert DL. Delivery of sphingosine 1 - phosphate from poly(ethylene glycol) hydrogels. Biomacromolecules. 2006; 7(4):1335–1343. [PubMed: 16602758]
128. Steffens GC, Yao C, Prevel P, Markowicz M, Schenck P, Noah EM, Pallua N. Modulation of angiogenic potential of collagen matrices by covalent incorporation of heparin and loading with vascular endothelial growth factor. Tissue Eng. 2004; 10(9–10):1502–1509. [PubMed: 15588409]
129. Chin WW, Lau WK, Bhuvaneswari R, Heng PW, Olivo M. Chlorin e6-polyvinylpyrrolidone as a fluorescent marker for fluorescence diagnosis of human bladder cancer implanted on the chick chorioallantoic membrane model. Cancer Lett. 2007; 245(1–2):127–133. [PubMed: 16516376]
130. Pegaz B, Debefve E, Ballini JP, Konan-Kouakou YN, van den Bergh H. Effect of nanoparticle size on the extravasation and the photothrombic activity of meso(p-tetracarboxyphenyl)porphyrin. J Photochem Photobiol B. 2006; 85(3):216–222. [PubMed: 16979346]
131. Yalcin M, Bharali DJ, Lansing L, Dyskin E, Mousa SS, Hercbergs A, Davis FB, Davis PJ, Mousa SA. Tetraidothyroacetic acid (tetrac) and tetrac nanoparticles inhibit growth of human renal cell carcinoma xenografts. Anticancer Res. 2009; 29(10):3825–3831. [PubMed: 19846915]
132. Howl J, Matou-Nasri S, West DC, Farquhar M, Slaninova J, Ostenson CG, Zorko M, Ostlund P, Kumar S, Langel U, McKeating J, Jones S. Bioportide: an emergent concept of bioactive cell-penetrating peptides. Cell Mol Life Sci. 2012; 69(17):2951–2966. [PubMed: 22527714]
133. Burt HM, Jackson JK, Bains SK, Liggins RT, Oktaba AM, Arsenault AL, Hunter WL. Controlled delivery of taxol from microspheres composed of a blend of ethylene-vinyl acetate copolymer and poly (d,l-lactic acid). Cancer Lett. 1995; 88(1):73–79. [PubMed: 7531612]

134. Murray J, Brown L, Langer R. Controlled release of microquantities of macromolecules. Cancer Drug Delivery. 1984; 1(2):119–123. [PubMed: 6544628]

135. Wutzler P, Sauerbrei A, Hartl A, Reimer K. Comparative testing of liposomal and aqueous formulations of povidone-iodine for their angioirritative potential at the chorioallantoic membrane of ex ovo cultivated chick embryos. Dermatology. 2003; 207(1):43–47. [PubMed: 12835547]

136. Kanczler JM, Barry J, Ginty P, Howdle SM, Shakesheff KM, Oreffo RO. Supercritical carbon dioxide generated vascular endothelial growth factor encapsulated poly(DL-lactic acid) scaffolds induce angiogenesis in vitro. Biochem Biophys Res Commun. 2007; 352(1):135–141. [PubMed: 17112464]

137. Wong C, Inman E, Spaethe R, Helgerson S. Fibrin-based biomaterials to deliver human growth factors. Thromb Haemost. 2003; 89(3):573–582. [PubMed: 12624643]

138. Jain K, Jain NK. Surface engineered dendrimers as antiangiogenic agent and carrier for anticancer drug: dual attack on cancer. J Nanosci Nanotechnol. 2014; 14(7):5075–5087. [PubMed: 24757983]

139. Klueh U, Dorsky DI, Kreutzer DL. Enhancement of implantable glucose sensor function in vivo using gene transfer-induced neovascularization. Biomaterials. 2005; 26(10):1155–1163. [PubMed: 15451635]

140. Madsen SJ, Sun CH, Tromberg BJ, Wallace VP, Hirschberg H. Photodynamic therap y of human glioma spheroids using 5-aminolevulinic acid. Photochem Photobiol. 2000; 72(1):128–134. [PubMed: 10911737]

141. Debefve E, Pegaz B, Ballini JP, van den Bergh H. Combination therapy using verteporfin and ranibizumab; optimizing the timing in the CAM model. Photochem Photobiol. 2009; 85(6):1400–1408. [PubMed: 19706144]

142. Zuluaga MF, Mailhos C, Robinson G, Shima DT, Gurny R, Lange N. Synergies of VEGF inhibition and photodynamic therapy in the treatment of age-related macular degeneration. Invest Ophthalmol Vis Sci. 2007; 48(4):1767–1772. [PubMed: 17389510]

143. Seymour RS, Wagner-Amos K. Non-invasive measurement of oxygen partial pressure, lateral diffusion and chorioallantoic blood flow under the avian eggshell. Comp Biochem Physiol A Mol Integr Physiol. 2008; 150(2):258–264. [PubMed: 16815717]

144. Huntosova V, Gay S, Nowak-Sliwinska P, Rajendran SK, Zellweger M, van den Bergh H, Wagnieres G. In vivo measurement of tissue oxygenation by time-resolved luminescence spectroscopy: advantageous properties of dichlorotris(1, 10-phenanthroline)-ruthenium(II) hydrate. J Biomed Opt. 2014; 19(7):77004. [PubMed: 25036215]

145. Debefve E, Cheng C, Schaefer SC, Yan H, Ballini JP, van den Bergh H, Lehr HA, Ruffieux C, Ris HB, Krueger T. Photodynamic therapy induces selective extravasation of macromolecules: Insights using intravital microscopy. J Photochem Photobiol B. 2010; 98(1):69–76. [PubMed: 20056552]

146. Wagnières, G.; Jichlinski, P.; Lange, N.; Kucera, P.; van den Bergh, H. From bench to bedside – the Hexvix® story. In: HMaS, S., editor. Handbook of Photomedicine. Taylor & Francis; 2013.

147. Malik E, Meyhofer-Malik A, Berg C, Bohm W, Kunzi-Rapp K, Diedrich K, Ruck A. Fluorescence diagnosis of endometriosis on the chorioallantoic membrane using 5-aminolaevulinic acid. Hum Reproduc. 2000; 15(3):584–588.

148. Saw CL, Olivo M, Chin WW, Soo KC, Heng PW. Superiority of N-methyl pyrrolidone over albumin with hypericin for fluorescence diagnosis of human bladder cancer cells implanted in the chick chorioallantoic membrane model. J Photochem Photobiol B. 2007; 86(3):207–218. [PubMed: 17134910]

149. Mondon K, Zeisser-Labouebe M, Gurny R, Moller M. MPEG-hexPLA micelles as novel carriers for hypericin, a fluorescent marker for use in cancer diagnostics. Photochem Photobiol. 2011; 87(2):399–407. [PubMed: 21166812]

150. Rees CJ, Allen J, Postma GN, Belafsky PC. Effects of Gold laser on the avian chorioallantoic membrane. Ann Otol Rhinol Laryngol. 2010; 119(1):50–53. [PubMed: 20128188]

151. Broadhurst MS, Akst LM, Burns JA, Kobler JB, Heaton JT, Anderson RR, Zeitels SM. Effects of 532 nm pulsed-KTP laser parameters on vessel ablation in the avian chorioallantoic membrane: implications for vocal fold mucosa. Laryngoscope. 2007; 117(2):220–225. [PubMed: 17204988]
152. Polytarchou C, Kardamakis D, Katsoris P, Papadimitriou E. Antioxidants modify the effect of X rays on blood vessels. Anticancer Res. 2006; 26(4B):3043–3047. [PubMed: 16886632]
153. Giannopoulou E, Katsoris P, Parthymou A, Kardamakis D, Papadimitriou E. Amifostine protects blood vessels from the effects of ionizing radiation. Anticancer Res. 2002; 22(5):2821–2826. [PubMed: 12530003]
154. Giannopoulou E, Katsoris P, Hatziapostolou M, Kardamakis D, Kotsaki E, Polytarchou C, Parthymou A, Papaioannou S, Papadimitriou E. X-rays modulate extracellular matrix in vivo. Int J Cancer. 2001; 94(5):690–698. [PubMed: 11745464]
155. Sabatasso S, Laissue JA, Hlushchuk R, Graber W, Bravin A, Brauer-Krisch E, Corde S, Blattmann H, Gruber G, Djonov V. Microbeam radiation-induced tissue damage depends on the stage of vascular maturation. Int J Radiat Oncol Biol Phys. 2011; 80(5):1522–1532. [PubMed: 21740994]
156. Gorski DH, Mauceri HJ, Salloum RM, Halpern A, Seetharam S, Weichselbaum RR. Prolonged treatment with angiostatin reduces metastatic burden during radiation therapy. Cancer Res. 2003; 63(2):308–311. [PubMed: 12543780]
157. Parthymou A, Kardamakis D, Pavlopoulos I, Papadimitriou E. Irradiated C6 glioma cells induce angiogenesis in vivo and activate endothelial cells in vitro. Int J Cancer. 2004; 110(6):807–814. [PubMed: 15170661]
158. Hatjikondi O, Ravazoula P, Kardamakis D, Dimopoulos J, Papaioannou S. In vivo experimental evidence that the nitric oxide pathway is involved in the X-ray-induced antiangiogenicity. Br J Cancer. 1996; 74(12):1916–1923. [PubMed: 8980390]
159. Hadjimichael C, Kardamakis D, Papaioannou S. Irradiation dose-response effects on angiogenesis and involvement of nitric oxide. Anticancer Res. 2005; 25(2A):1059–1065. [PubMed: 15868946]
160. Kanthou C, Tozer GM. Microtubule depolymerizing vascular disrupting agents: novel therapeutic agents for oncology and other pathologies. Int J Exp Pathol. 2009; 90(3):284–294. [PubMed: 19563611]
161. Galbraith SM, Chaplin DJ, Lee F, Stratford MR, Locke RJ, Vojnovic B, Tozer GM. Effects of combretastatin A4 phosphate on endothelial cell morphology in vitro and relationship to tumour vascular targeting activity in vivo. Anticancer Res. 2001; 21(1A):93–102. [PubMed: 11299795]
162. Mahal K, Resch M, Ficner R, Schobert R, Biersack B, Mueller T. Effects of the tumor-vasculature-disrupting agent verubulin and two heteroaryl analogues on cancer cells, endothelial cells, and blood vessels. ChemMedChem. 2014; 9(4):847–854. [PubMed: 24678059]
163. Ren X, Dai M, Lin LP, Li PK, Ding J. Anti-angiogenic and vascular disrupting effects of C9, a new microtubule-depolymerizing agent. Brit J Pharmacol. 2009; 156(8):1228–1238. [PubMed: 19302593]
164. Petitclerc E, Deschesnes RG, Cote MF, Marquis C, Janvier R, Lacroix J, Miot-Noirault E, Legault J, Mounetou E, Madelmont JC, R CG. Antiangiogenic and antitumoral activity of phenyl-3-(2-chloroethyl)ureas: a class of soft alkylating agents disrupting microtubules that are unaffected by cell adhesion-mediated drug resistance. Cancer Res. 2004; 64(13):4654–4663. [PubMed: 15231678]
165. Jiang Z, Wu M, Miao J, Duan H, Zhang S, Chen M, Sun L, Wang Y, Zhang X, Zhu X, Zhang L. Deoxypodophyllotoxin exerts both anti-angiogenic and vascular disrupting effects. Int J Biochem Cell Biol. 2013; 45(8):1710–1719. [PubMed: 23702033]
166. Ribatti D, Guidolin D, Conconi MT, Nico B, Baiguera S, Parnigotto PP, Vacca A, Nussdorfer GG. Vinblastine inhibits the angiogenic response induced by adrenomedullin in vitro and in vivo. Oncogene. 2003; 22(41):6458–6461. [PubMed: 14508526]
167. Muenzner JK, Biersack B, Kalie H, Andronache IC, Kaps L, Schuppan D, Sasse F, Schobert R. Gold(I) Biscarbene Complexes Derived from Vascular-Disrupting Combretastatin A-4 Address Different Targets and Show Antimetastatic Potential. ChemMedChem. 2014; 9(6):1195–204. [PubMed: 24648184]

168. Vargas A, Zeisser-Labouebe M, Lange N, Gurny R, Delie F. The chick embryo and its chorioallantoic membrane (CAM) for the in vivo evaluation of drug delivery systems. Adv Drug Deliver Rev. 2007; 59(11):1162–1176.

169. Ehrbar M, Djonov VG, Schnell C, Tschanz SA, Martiny-Baron G, Schenk U, Wood J, Burri PH, Hubbell JA, Zisch AH. Cell-demanded liberation of VEGF121 from fibrin implants induces local and controlled blood vessel growth. Circ Res. 2004; 94(8):1124–1132. [PubMed: 15044320]

170. Vargas A, Zeisser-Labouebe M, Lange N, Gurny R, Delie F. The chick embryo and its chorioallantoic membrane (CAM) for the in vivo evaluation of drug delivery systems. Adv Drug Deliver Rev. 2007; 59(11):1162–1176.

171. Ismail MS, Torsten U, Dressler C, Diederichs JE, Huske S, Weitzel H, Berlien HP. Photodynamic Therapy of Malignant Ovarian Tumours Cultivated on CAM. Lasers Med Sci. 1999; 14(2):91–96. [PubMed: 24519162]

172. Romanoff, AL. The Avian Embryo: structural and functional development. McMillan; New York: 1960.

173. Ling TY, Liu YL, Huang YK, Gu SY, Chen HK, Ho CC, Tsao PN, Tung YC, Chen HW, Cheng CH, Lin KH, Lin FH. Differentiation of lung stem/progenitor cells into alveolar pneumocytes and induction of angiogenesis within a 3D gelatin - Microbubble scaffold. Biomaterials. 2014; 35(22):5660–5669. [PubMed: 24746968]

174. Noiman T, Buzhor E, Metsuyanim S, Harari-Steinberg O, Morgenshtern C, Dekel B, Goldstein RS. A rapid in vivo assay system for analyzing the organogenetic capacity of human kidney cells. Organogenesis. 2011; 7(2):140–144. [PubMed: 21613816]

175. Klueh U, Dorsky DI, Moussy F, Kreutzer DL. Ex ova chick chorioallantoic membrane as a novel model for evaluation of tissue responses to biomaterials and implants. J Biomed Mater Res Part A. 2003; 67(3):838–843.

176. Bronckaers A, Hilkens P, Fanton Y, Struys T, Gervois P, Politis C, Martens W, Lambrichts I. Angiogenic properties of human dental pulp stem cells. PLoS One. 2013; 8(8):e71104. [PubMed: 23951091]

177. 404: Acute Dermal Irritation/Corrosion. OECD Guideline for the Testing of Chemicals OECD Publishing. 2012

178. Scheel J, Heppenheimer A, Lehringer E, Kreutz J, Poth A, Ammann H, Reisinger K, Banduhn N. Classification and labeling of industrial products with extreme pH by making use of in vitro methods for the assessment of skin and eye irritation and corrosion in a weight of evidence approach. Toxicol in vitro. 2011; 25(7):1435–1447. [PubMed: 21550395]

179. Kunzi-Rapp K, Ruck A, Kaufmann R. Characterization of the chick chorioallantoic membrane model as a short-term in vivo system for human skin. Arch Dermatol Res. 1999; 291(5):290–295. [PubMed: 10367712]

180. Slodownik D, Grinberg I, Spira RM, Skornik Y, Goldstein RS. The human skin/chick chorioallantoic membrane model accurately predicts the potency of cosmetic allergens. Expl Dermatol. 2009; 18(4):409–413.

181. Li J, Tripathi RC, Tripathi BJ. Drug-induced ocular disorders. Drug Saf. 2008; 31(2):127–141. [PubMed: 18217789]

182. Short BG. Safety evaluation of ocular drug delivery formulations: techniques and practical considerations. Toxicol Pathol. 2008; 36(1):49–62. [PubMed: 18337221]

183. Saw CL, Heng PW, Liew CV. Chick chorioallantoic membrane as an in situ biological membrane for pharmaceutical formulation development: a review. Drug Dev Ind Pharm. 2008; 34(11): 1168–1177. [PubMed: 18663656]

184. Alany RG, Rades T, Nicoll J, Tucker IG, Davies NM. W/O microemulsions for ocular delivery: evaluation of ocular irritation and precorneal retention. J Control Release. 2006; 111(1–2):145–152. [PubMed: 16426694]

185. Luepke NP. Hen's egg chorioallantoic membrane test for irritation potential. Food Chem Toxicol. 1985; 23(2):287–291. [PubMed: 4040077]

186. Barile FA. Validating and troubleshooting ocular in vitro toxicology tests. J Pharmacol Toxicol Meth. 2010; 61(2):136–145.

187. Abdelkader H, Ismail S, Hussein A, Wu Z, Al-Kassas R, Alany RG. Conjunctival and corneal tolerability assessment of ocular naltrexone niosomes and their ingredients on the hen's egg chorioallantoic membrane and excised bovine cornea models. Int J Pharm. 2012; 432(1–2):1–10. [PubMed: 22575752]

188. Debbasch C, Ebenhahn C, Dami N, Pericoi M, Van den Berghe C, Cottin M, Nohynek GJ. Eye irritation of low-irritant cosmetic formulations: correlation of in vitro results with clinical data and product composition. Food Chem Toxicol. 2005; 43(1):155–165. [PubMed: 15582208]

189. Hagino S, Kinoshita S, Tani N, Nakamura T, Ono N, Konishi K, Iimura H, Kojima H, Ohno Y. Interlaboratory validation of in vitro eye irritation tests for cosmetic ingredients. (2) Chorioallantoic membrane (CAM) test. Toxicol in vitro. 1999; 13(1):99–113. [PubMed: 20654469]

190. Leng T, Miller JM, Bilbao KV, Palanker DV, Huie P, Blumenkranz MS. The chick chorioallantoic membrane as a model tissue for surgical retinal research and simulation. Retina. 2004; 24(3):427–434. [PubMed: 15187666]

191. Guttman Krader C, Laudererdale F. New innovations. Eurotimes. 2013; 18(3):34–34.

192. Ullrich F, Bergeles C, Pokki J, Ergeneman O, Erni S, Chatzipirpiridis G, Pane S, Framme C, Nelson BJ. Mobility Experiments with Microrobots for Minimally Invasive Intraocular Surgery. Invest Ophthalmol Vis Sci. 2013; 54(4):2853–63. [PubMed: 23518764]

193. Murphy JB. The Effect of Adult Chicken Organ Grafts on the Chick Embryo. J Exp Med. 1916; 24(1):1–5. [PubMed: 19868024]

194. Chiba A, Yui C, Hirano S. Liver reconstruction on the chorioallantoic membrane of the chick embryo. Arch Histol Cytol. 2010; 73(1):45–53. [PubMed: 21471666]

195. Maas JW, Le Noble FA, Dunselman GA, de Goeij AF, Struyker Boudier HA, Evers JL. The chick embryo chorioallantoic membrane as a model to investigate the angiogenic properties of human endometrium. Gynecol Obstet Invest. 1999; 48(2):108–112. [PubMed: 10461001]

196. Bertossi M, Virgintino D, Coltey P, Errede M, Mancini L, Roncali L. Angiogenesis and endothelium phenotype expression in embryonic adrenal gland and cerebellum grafted onto chorioallantoic membrane. Angiogenesis. 1999; 3(4):305–315. [PubMed: 14517410]

197. Katoh M, Nakada K, Miyazaki JI. Liver regeneration on chicken chorioallantoic membrane. Cells Tissues Organs. 2001; 169(2):125–133. [PubMed: 11399852]

198. Lemon G, Howard D, Tomlinson MJ, Buttery LD, Rose FR, Waters SL, King JR. Mathematical modelling of tissue-engineered angiogenesis. Math Biosci. 2009; 221(2):101–120. [PubMed: 19619562]

199. Eugenin J, Eyzaguirre C. Electrophysiological properties of rat nodose ganglion neurons co-transplanted with carotid bodies into the chick chorioallantoic membrane. Biol Res. 2005; 38(4): 329–334. [PubMed: 16579513]

200. Yang XB, Whitaker MJ, Sebald W, Clarke N, Howdle SM, Shakesheff KM, Oreffo RO. Human osteoprogenitor bone formation using encapsulated bone morphogenetic protein 2 in porous polymer scaffolds. Tissue Eng. 2004; 10(7–8):1037–1045. [PubMed: 15363161]

201. Vargas GE, Mesones RV, Bretcanu O, Lopez JM, Boccaccini AR, Gorustovich A. Biocompatibility and bone mineralization potential of 45S5 Bioglass-derived glass-ceramic scaffolds in chick embryos. Acta Biomater. 2009; 5(1):374–380. [PubMed: 18706880]

202. Buschmann J, Welti M, Hemmi S, Neuenschwander P, Baltes C, Giovanoli P, Rudin M, Calcagni M. Three-dimensional co-cultures of osteoblasts and endothelial cells in DegraPol foam: histological and high-field magnetic resonance imaging analyses of pre-engineered capillary networks in bone grafts. Tissue Eng Part A. 2011; 17(3–4):291–299. [PubMed: 20799888]

203. Navarro M, DeRuiter MC, Carretero A, Ruberte J. Microvascular assembly and cell invasion in chick mesonephros grafted onto chorioallantoic membrane. J Anat. 2003; 202(2):213–225. [PubMed: 12647871]

204. Ko HC, Milthorpe BK, McFarland CD. Engineering thick tissues-the vascularisation problem. Eur Cell Mater. 2007; 14:1–18. discussion 18–19. [PubMed: 17654452]

205. Verhoelst E, De Ketelaere B, Bruggeman V, Villamor E, Decuypere E, De Baerdemaeker J. Development of a fast, objective, quantitative methodology to monitor angiogenesis in the

chicken chorioallantoic membrane during development. Int J Dev Biol. 2011; 55(1):85–92. [PubMed: 21425083]

206. Verhoelst E, De Ketelaere B, Decuypere E, De Baerdemaeker J. The effect of early prenatal hypercapnia on the vascular network in the chorioallantoic membrane of the chicken embryo. Biotechnol Progr. 2011; 27(2):562–570.
207. Warren CM, Ziyad S, Briot A, Der A, Iruela-Arispe ML. A ligand-independent VEGFR2 signaling pathway limits angiogenic responses in diabetes. Sci Signal. 2014; 7(307):ra1. [PubMed: 24399295]
208. Ribatti D, Cruz A, Nico B, Favier J, Vacca A, Corsi P, Roncali L, Dammacco F. In situ hybridization and immunogold localization of vascular endothelial growth factor receptor-2 on the pericytes of the chick chorioallantoic membrane. Cytokine. 2002; 17(5):262–265. [PubMed: 12027407]
209. Ribatti D, Nico B, Vacca A, Roncali L. Localization of factor VIII-related antigen in the endothelium of the chick embryo chorioallantoic membrane. Histochem Cell Biol. 1999; 112(6): 447–450. [PubMed: 10651095]
210. Ribatti D, Nico B, Vacca A, Iurlaro M, Roncali L. Temporal expression of the matrix metalloproteinase MMP-2 correlates with fibronectin immunoreactivity during the development of the vascular system in the chick embryo chorioallantoic membrane. J Anat. 1999; 195(Pt 1): 39–44. [PubMed: 10473291]
211. Iruela-Arispe ML, Lane TF, Redmond D, Reilly M, Bolender RP, Kavanagh TJ, Sage EH. Expression of SPARC during development of the chicken chorioallantoic membra ne: evidence for regulated proteolysis in vivo. Mol Biol Cell. 1995; 6(3):327–343. [PubMed: 7612967]
212. Flamme I, Schulze-Osthoff K, Jacob HJ. Mitogenic activity of chicken chorioallantoic fluid is temporally correlated to vascular growth in the chorioallantoic membrane a nd related to fibroblast growth factors. Development. 1991; 111(3):683–690. [PubMed: 1879335]
213. Moyon D, Pardanaud L, Yuan L, Breant C, Eichmann A. Plasticity of endothelial cells during arterial-venous differentiation in the avian embryo. Development. 2001; 128(17):3359–3370. [PubMed: 11546752]
214. Schughart K, Accart N. Use of adenovirus vectors for functional gene analysis in the chicken chorioallantoic membrane. BioTechniques. 2003; 34(1):178–183. [PubMed: 12545557]
215. Forough R, Weylie B, Patel C, Ambrus S, Singh US, Zhu J. Role of AKT/PKB signaling in fibroblast growth factor-1 (FGF-1)-induced angiogenesis in the chicken chorioallantoic membrane (CAM). J Cell Biochem. 2005; 94(1):109–116. [PubMed: 15517595]
216. Druyan S, Levi E. Reduced O2 concentration during CAM development–its effect on angiogenesis and gene expression in the broiler embryo CAM. Gene Expr Patterns. 2012; 12(7–8):236–244. [PubMed: 22609957]
217. Strick DM, Waycaster RL, Montani JP, Gay WJ, Adair TH. Morphometric measurements of chorioallantoic membrane vascularity: effects of hypoxia and hyperoxia. Am J Physiol. 1991; 260(4 Pt 2):H1385–1389. [PubMed: 2012235]
218. Burton GJ, Palmer ME. Development of the chick chorioallantoic capillary plexus under normoxic and normobaric hypoxic and hyperoxic conditions: a morphometric study. J Exp Zool. 1992; 262(3):291–298. [PubMed: 1640200]
219. Baum O, Suter F, Gerber B, Tschanz SA, Buergy R, Blank F, Hlushchuk R, Djonov V. VEGF-A promotes intussusceptive angiogenesis in the developing chicken chorioallantoic membrane. Microcirculation. 2010; 17(6):447–457. [PubMed: 20690983]
220. Schlatter P, Konig MF, Karlsson LM, Burri PH. Quantitative study of intussusceptive capillary growth in the chorioallantoic membrane (CAM) of the chicken embryo. Microvasc Res. 1997; 54(1):65–73. [PubMed: 9245646]
221. Patan S, Haenni B, Burri PH. Implementation of intussusceptive microvascular growth in the chicken chorioallantoic membrane (CAM). Microvasc Res. 1997; 53(1):33–52. [PubMed: 9056474]
222. Chouinard-Pelletier G, Leduc M, Guay D, Coulombe S, Leask RL, Jones EA. Use of inert gas jets to measure the forces required for mechanical gene transfection. Biomed Eng Online. 2012; 11:67. [PubMed: 22963645]

223. Lee GS, Filipovic N, Miele LF, Lin M, Simpson DC, Giney B, Konerding MA, Tsuda A, Mentzer SJ. Blood flow shapes intravascular pillar geometry in the chick chorioallantoic membrane. J Angiogenes Res. 2010; 2:11. [PubMed: 20609245]

224. Paulis YW, Soetekouw PM, Verheul HM, Tjan-Heijnen VC, Griffioen AW. Signalling pathways in vasculogenic mimicry. Biochim Biophys Acta. 2010; 1806(1):18–28. [PubMed: 20079807]

225. Branum SR, Yamada-Fisher M, Burggren W. Reduced heart rate and cardiac output differentially affect angiogenesis, growth, and development in early chicken embryos (Gallus domesticus). Physiol Biochem Zool. 2013; 86(3):370–382. [PubMed: 23629887]

226. le Noble F, Moyon D, Pardanaud L, Yuan L, Djonov V, Matthijsen R, Breant C, Fleury V, Eichmann A. Flow regulates arterial-venous differentiation in the chick embryo yolk sac. Development. 2004; 131(2):361–375. [PubMed: 14681188]

227. Matthews BD, Overby DR, Mannix R, Ingber DE. Cellular adaptation to mechanical stress: role of integrins, Rho, cytoskeletal tension and mechanosensitive ion channels. J Cell Sci. 2006; 119(Pt 3):508–518. [PubMed: 16443749]

228. Kumar S, Maxwell IZ, Heisterkamp A, Polte TR, Lele TP, Salanga M, Mazur E, Ingber DE. Viscoelastic retraction of single living stress fibers and its impact on cell shape, cytoskeletal organization, and extracellular matrix mechanics. Biophys J. 2006; 90(10):3762–3773. [PubMed: 16500961]

229. Moore KA, Polte T, Huang S, Shi B, Alsberg E, Sunday ME, Ingber DE. Control of basement membrane remodeling and epithelial branching morphogenesis in embryonic lung by Rho and cytoskeletal tension. Dev Dynam. 2005; 232(2):268–281.

230. Kilarski WW, Samolov B, Petersson L, Kvanta A, Gerwins P. Biomechanical regulation of blood vessel growth during tissue vascularization. Nat Med. 2009; 15(6):657–664. [PubMed: 19483693]

231. Mentzler, SJ. http://www.mentzerlab.org/images.html

232. Ruck A, Bohmler A, Steiner R. PDT with TOOKAD® studied in the chorioallantoic membrane of fertilized eggs. Photodiagn Photodyn Ther. 2005; 2(1):79–90.

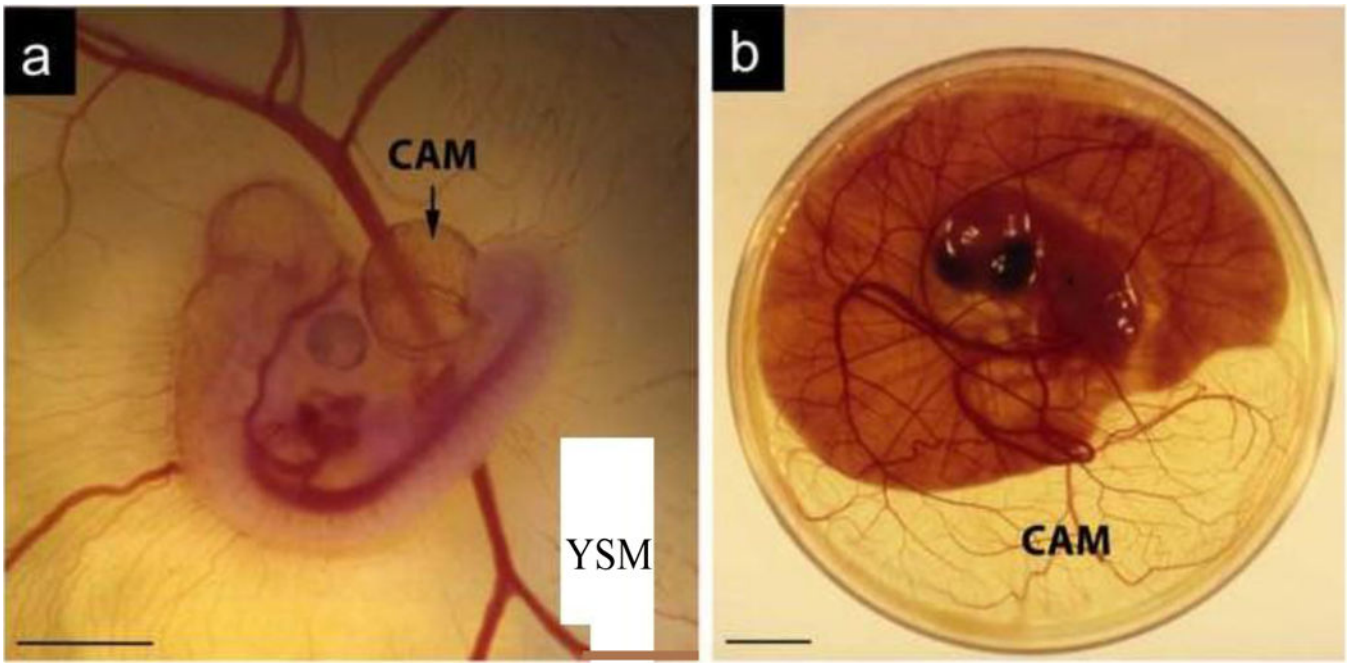

Figure 1.

Chicken embryo and associated extra-embryonic structures. **a** Chicken embryo at day 4 post-fertilization. Note the highly vascularized chorioallantoic membrane (CAM) that expands from the hind-gut. The yolk sac membrane (YSM), also highly vascularized, is seen in the background; **b** Embryo at day 12 post-fertilization into a 10 cm petri dish. Note the significant growth of the CAM that now exceeds the area covered by the yolk. The YSM is also present, but under the embryo and only associated with the yolk.

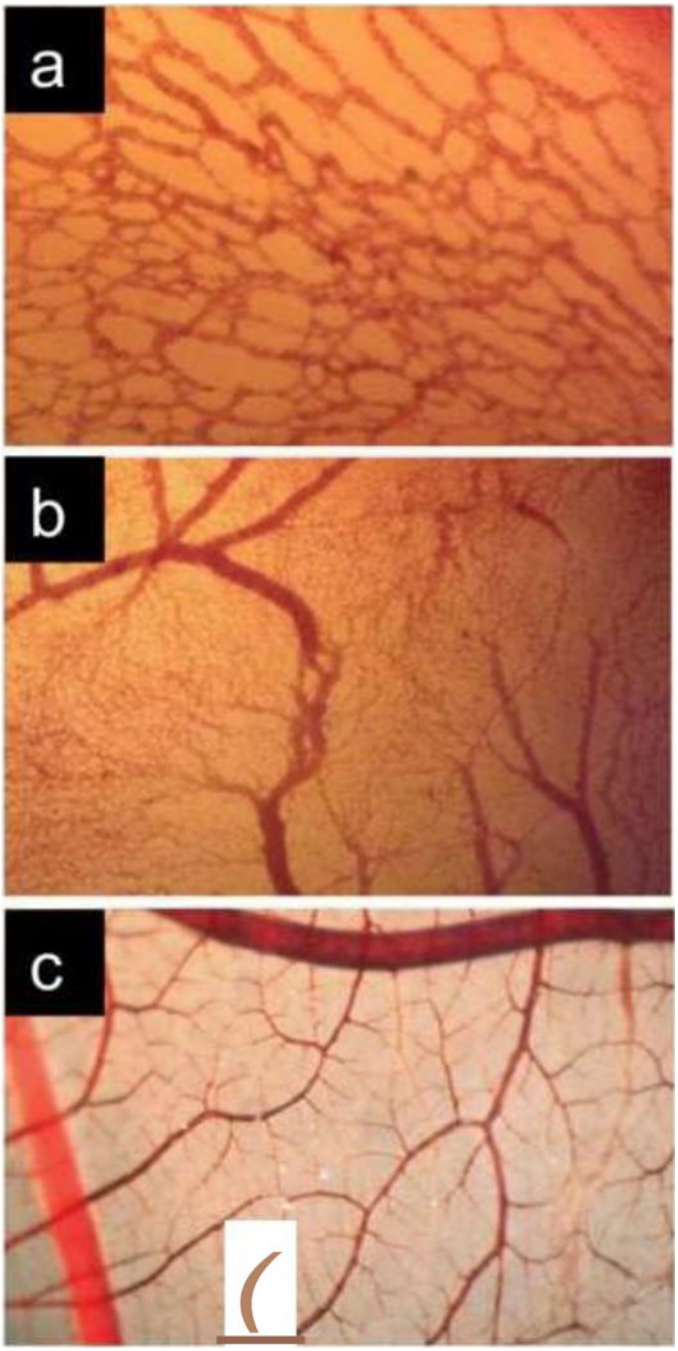

Figure 2.

Images illustrating the maturation of the CAM vasculature. **a** Primitive vascular plexus at day 3 post-fertilization; **b** Vascular remodeling, growth and anastomosis can be seen at day 7 post-fertilization; **c** Hierarchic vascular structures and fully differentiated vessels are noted at embryo development day 10.

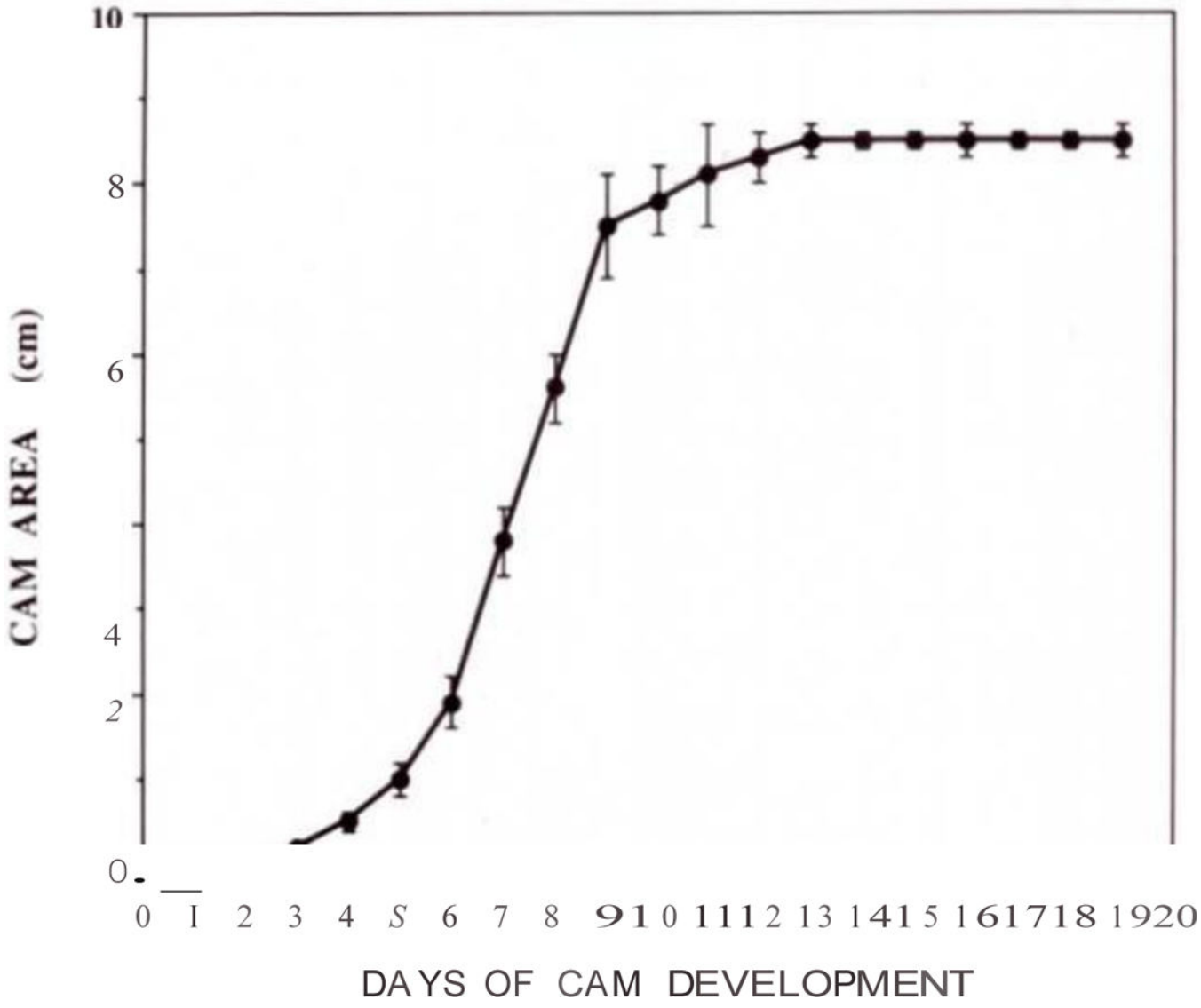

Figure 3.

Expansion of the CAM was measured daily. Graph shows the average of 5–7 CAMs per time point after plating the fertilized eggs into a 10 cm petri dish (+/− SD). Note the exponential growth between days 3 and 10.

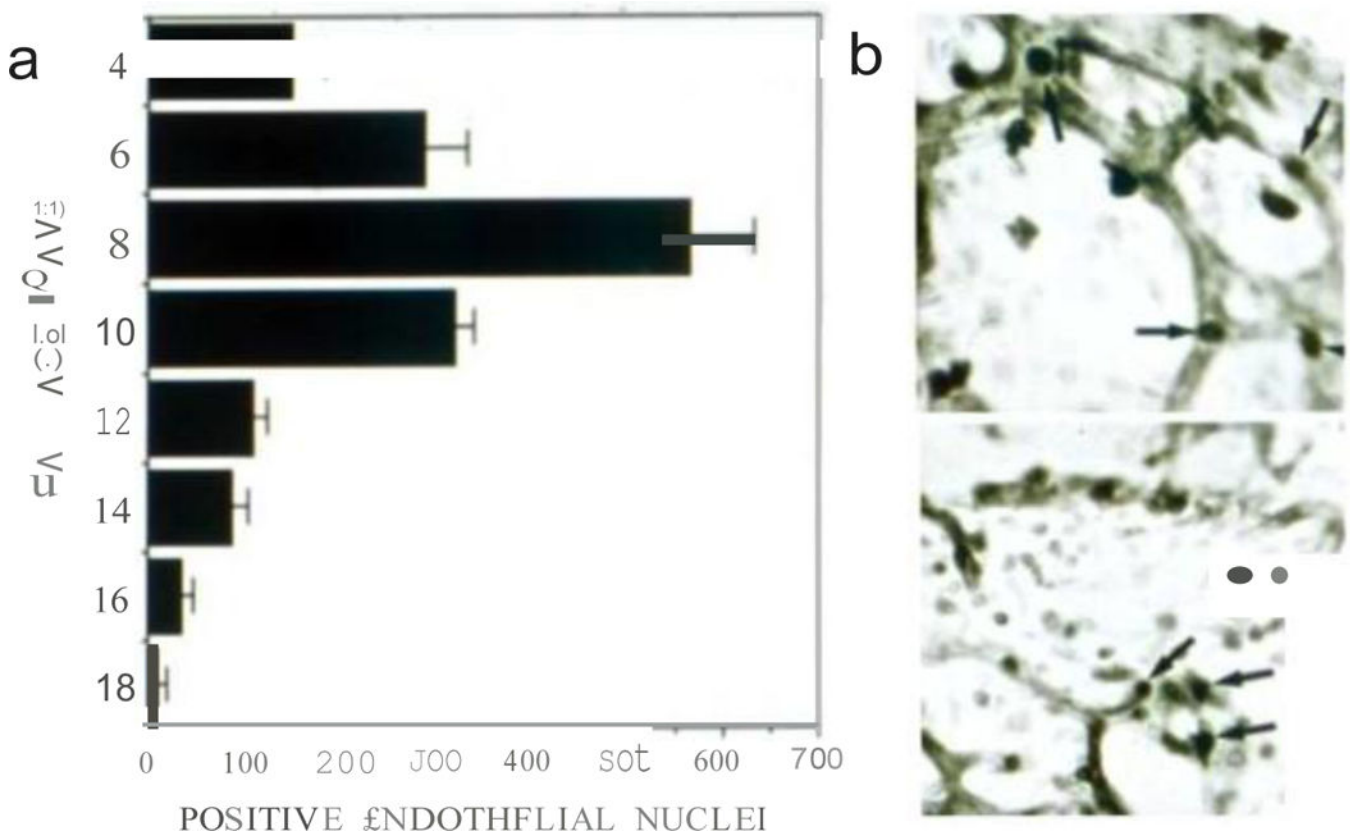

Figure 4.

Proliferation kinetics of CAM vessels. **a** Quantification of BrdU incorporation in CAM vessels at the indicated days post-fertilization. Counts per time point were the average of positive nuclei in the vessels from 3–4 CAMs per time point; **b** Example of images used to obtain the measurements. The upper panel represents embryo development at day 4 and lower panel is an example of embryo development at day 6.

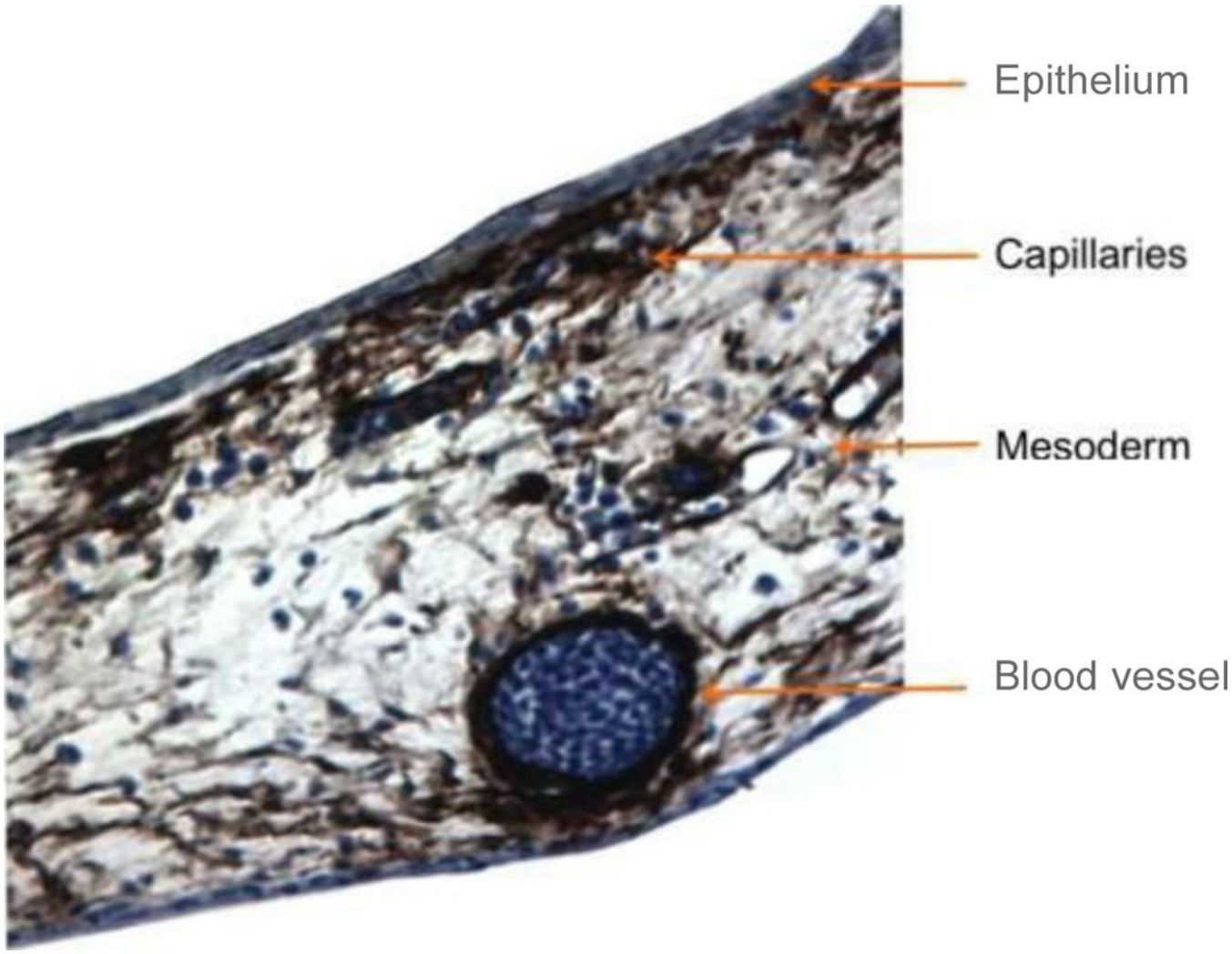

Figure 5.
Immunohistochemical visualization of α-smooth muscle actin (dark brown) in a transversal CAM section. Smaller capillary plexus is more superficial in comparison to the larger vessels located deeper in the CAM.

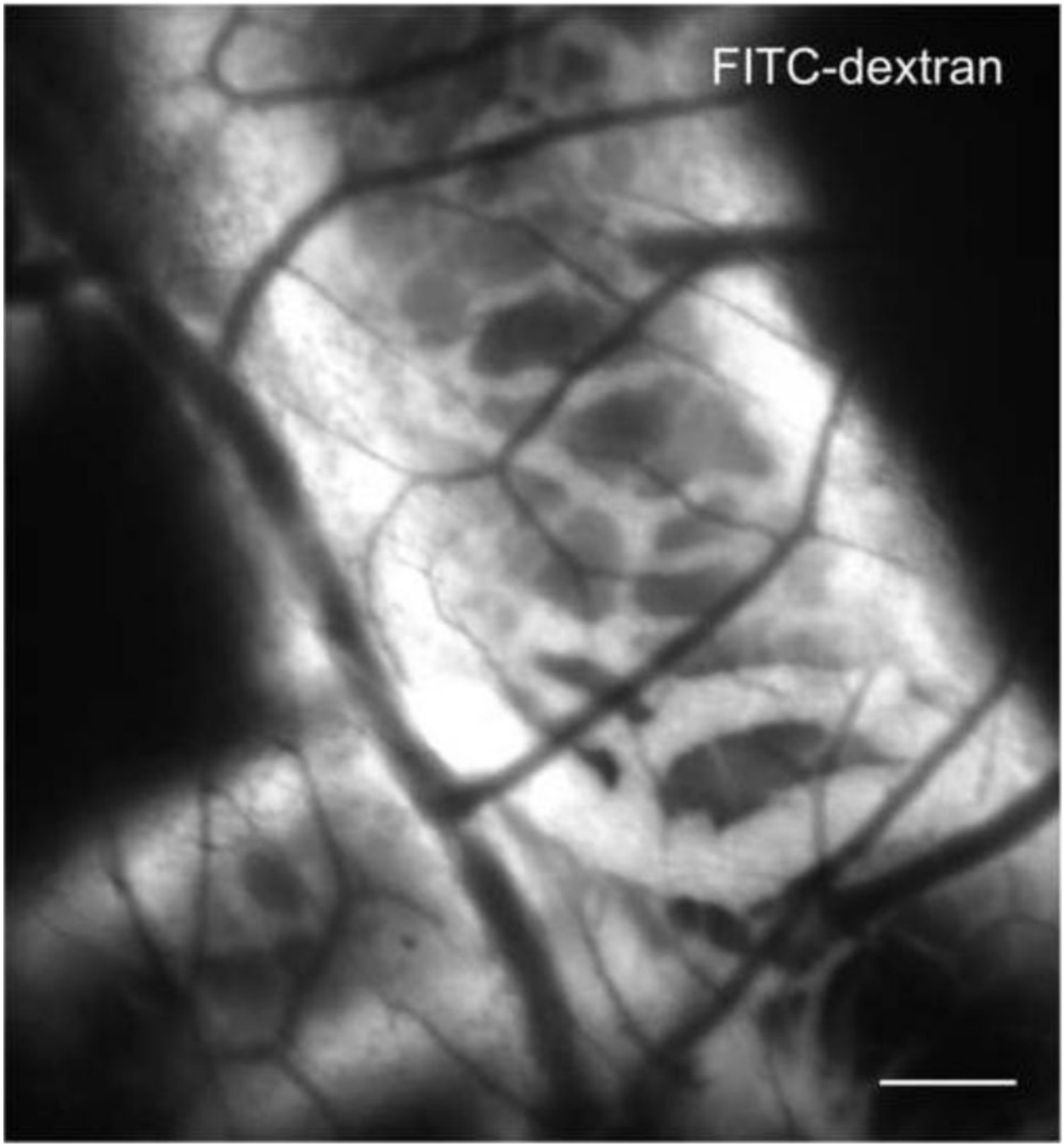

Figure 6.

Angiogram of the CAM lymphatic system. Lymphatic vessels around a large blood vessel were visualized by FITC-dextran fluorescence angiography (25 mg/kg; 20 kDa, λ_{ex} = 470 ± 20 nm). At a more superficial plane small non-fluorescent blood vessels are also visible. Bar = 20 μm.

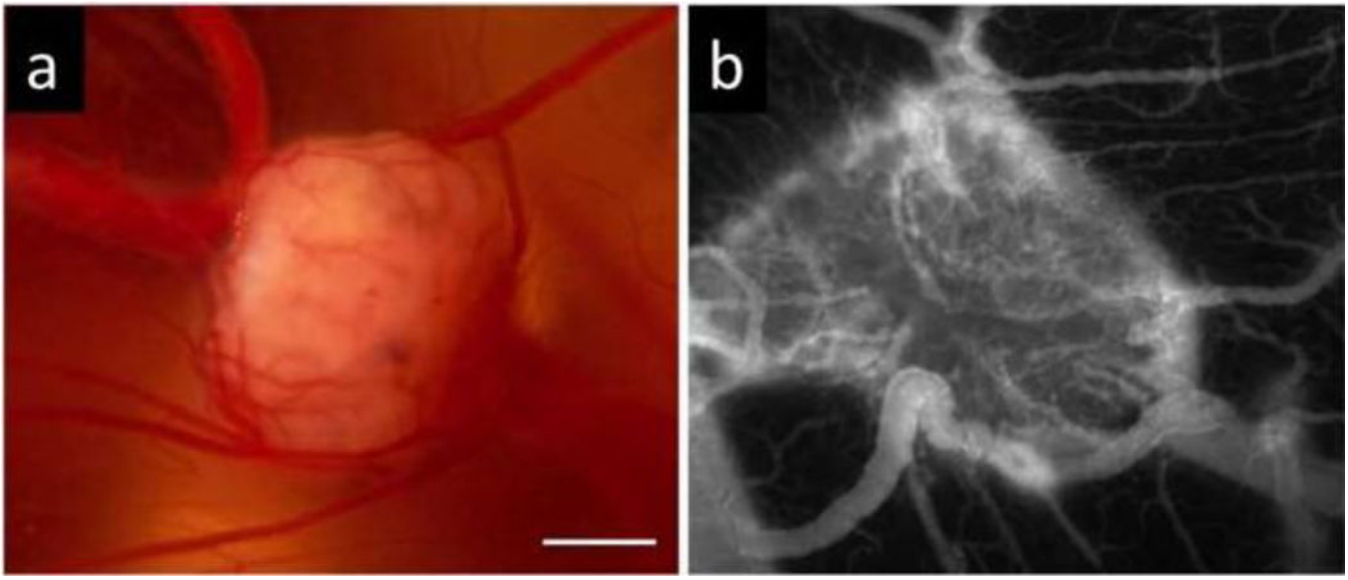

Figure 7.

Images of human A2780 ovarian carcinoma grown on the CAM. **a** Bright field image; **b** Fluorescence angiography (FITC-dextran, λ_{ex} = 470 ± 20 nm, λ_{em} = 520 nm). Functional vasculature of the CAM is integrated well in the tumor. Bar = 1 mm.

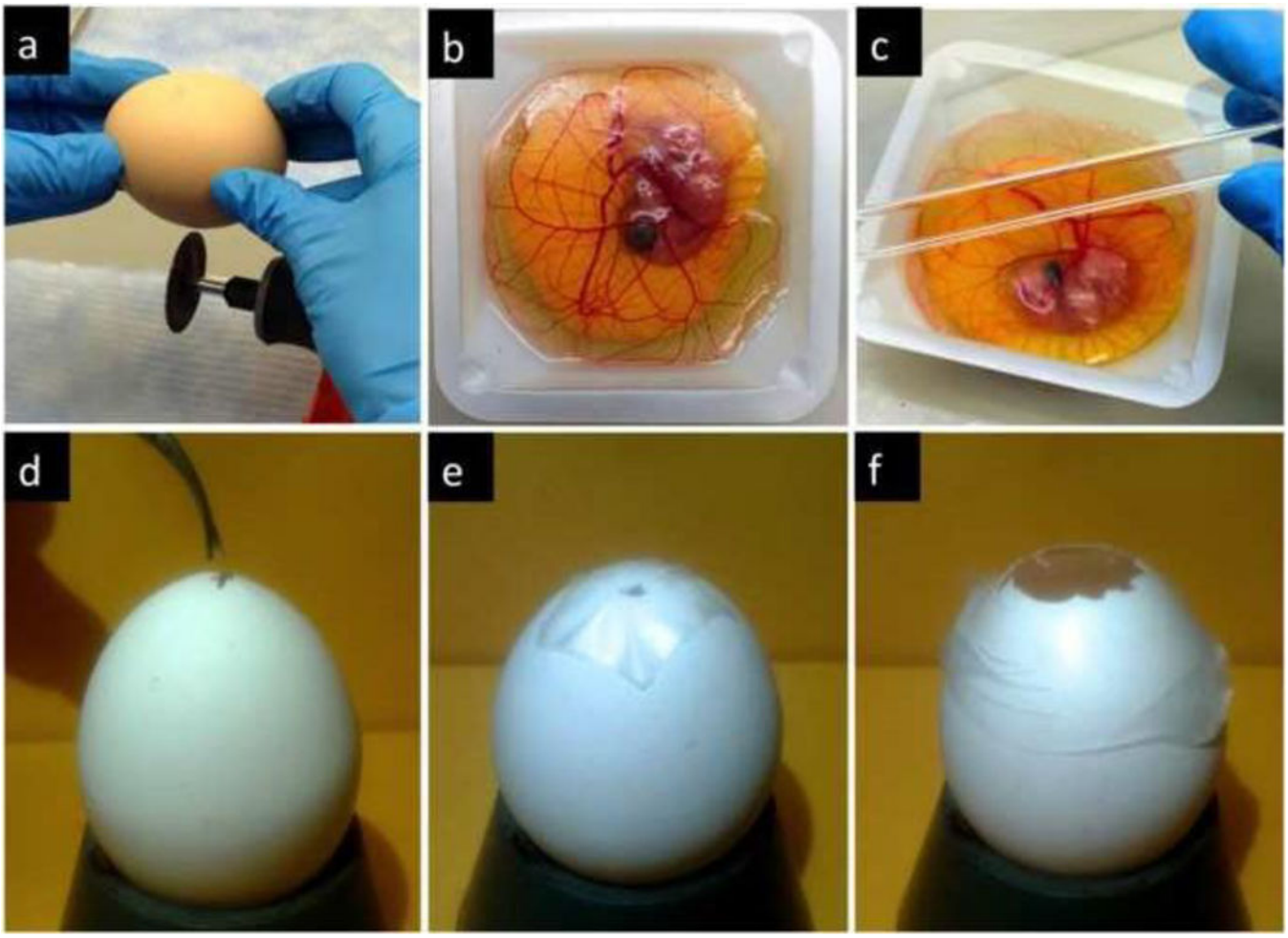

Figure 8.

CAM cultivation protocols. The e*x ovo* protocol (**a–c**) requires (**a**) a gentle cracking of the egg using a blade and transferring of the contents into a petri dish or weighing boats (**b**) with plastic a plastic cover (**c**). The *in ovo* cultivation (**d–f**) starts with gentle rotation for 3 days. On embryo development day 3 the eggshell is opened with a sterile tweezers (**d**) and subsequently covered with a laboratory wrapping film (**e**). On the day when the experiment starts, the shell above the air pouch of the egg is extended to a diameter of approximately 3 cm (**f**) enabling further experimental manipulation.

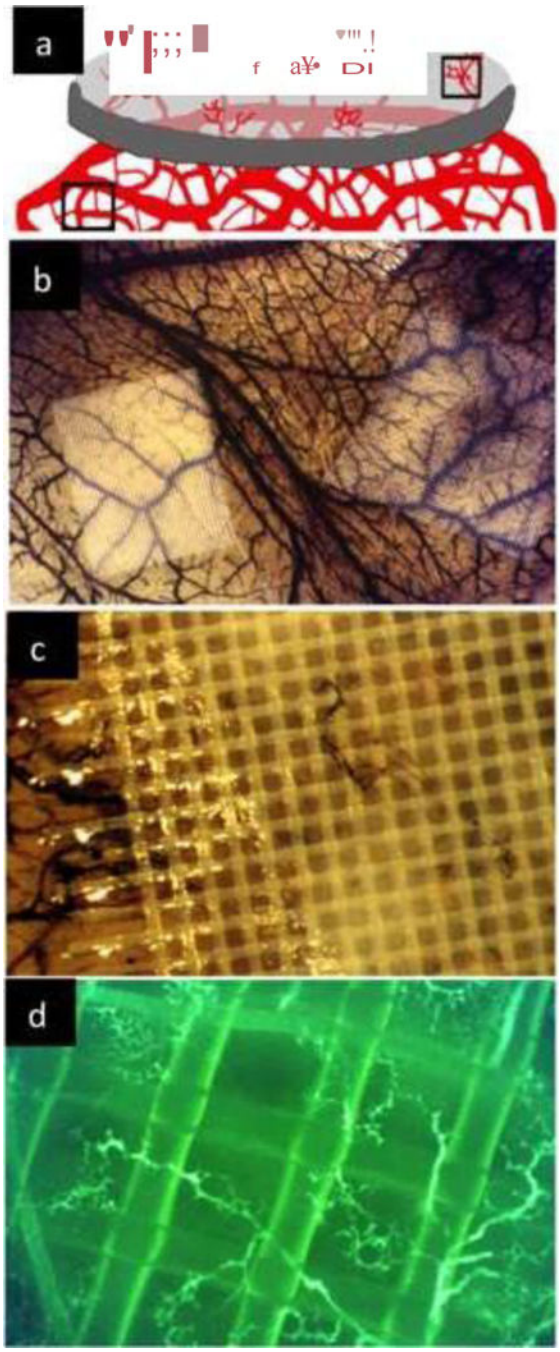

Figure 9.

Angiogenesis assays in the CAM. **a** Scheme of angiogenic growth into an avascular matrix. This assay requires growth against gravity and invasion into specific polymerized extracellular matrices. A variety of matrices can be used for this purpose; **b** Nylon mesh squares (pore size 250 μm; Tetko Inc) supporting a polymerized collagen gel containing FGF2 were placed on top of the CAM. The matrix on the left includes, in addition to FGF2, an anti-angiogenic factor (Thrombospondin1) the one on the right has a mixture of FGF2 and VEGF. The CAM was injected with india ink to visualized small vessels; **c** Higher

magnification showing the small vessel inside the previously avascular matrix; **d** The CAM can also be injected with dextran-FITC to visualize angiogenic vessels.

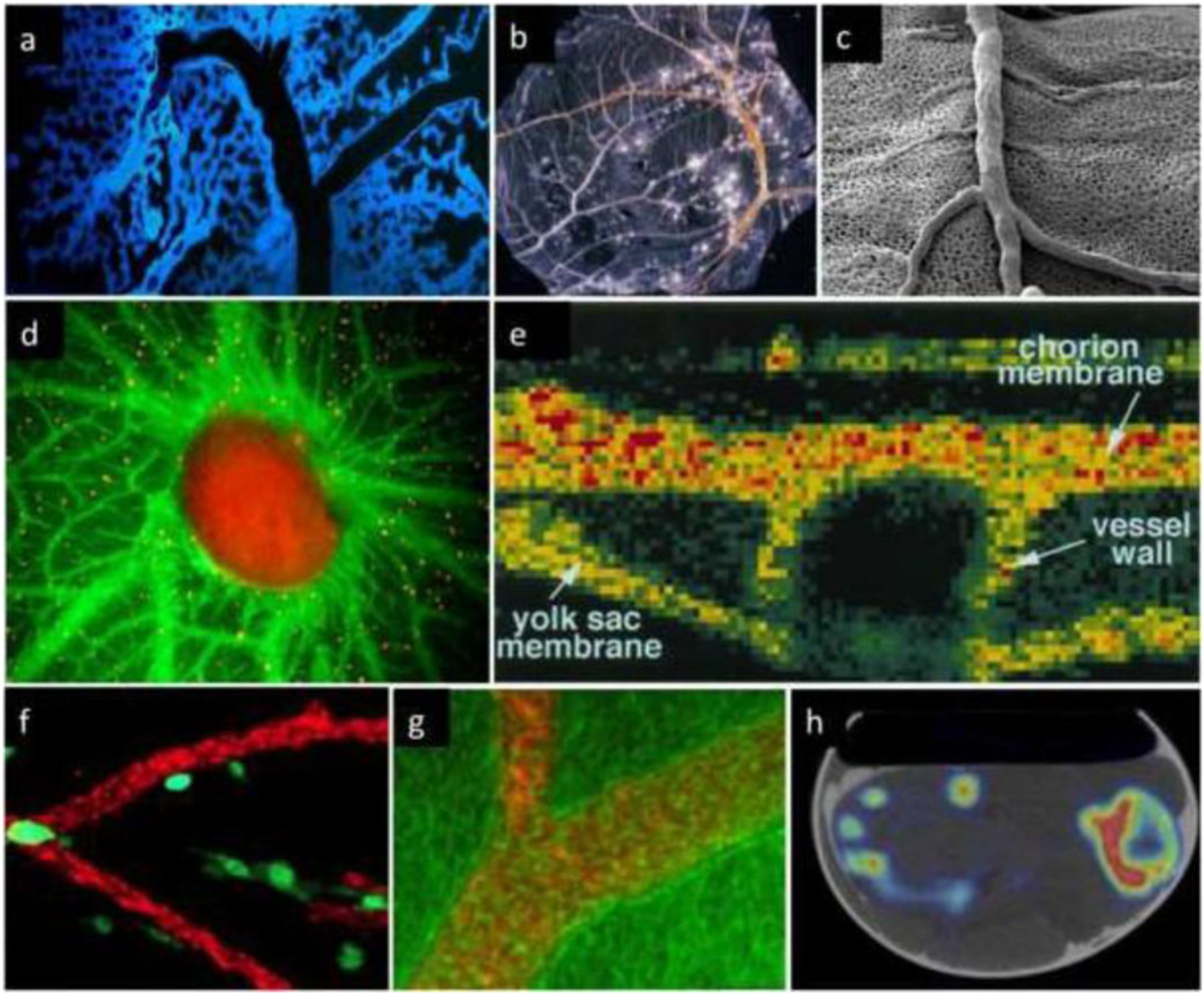

Figure 10.

Selected imaging techniques used to visualize the CAM vasculature of chicken embryo. **a** Confocal microscopy after blue fluorescent polymer injection, by Dr. Grace Lee and Dr. Steven, with permission from Mentzer's lab [231]; **b** light microscopy of Smallpox virus pocks on the CAM (from Public Health Image Library); **c** Scanning electron microscopy (unpublished data, courtesy of Dr. Valentin Djonov, Bern, Switzerland); **d** fluorescence microscopy (with green fluorescent plasma marker and orange fluorescent flow tracers), by Dr. Kenji Chamoto and Dr. Steven Mentzer, with permission from Mentzer's lab [231]; **e** non-invasive imaging of *in vivo* blood flow velocity using optical Doppler tomography, with permission from Chen et al [48]; **f** Cells escaping CAM primary tumors were visualized in the embryos with the vasculature highlighted with red fluorescent-tagged LCA, with permission from Springer [73]; **g** Fluorescence (red) distribution in the vessels by means of laser scanning microscopy (phase contrast image (green), with permission from Elsevier [232]; **h** co-registered PET and CT images of a chicken embryo in the shell after ^{18}F-Na

injection, with permission. This research was originally published in JNM. Warnock et al. [55]. © by the Society of Nuclear Medicine and Molecular Imaging, Inc.

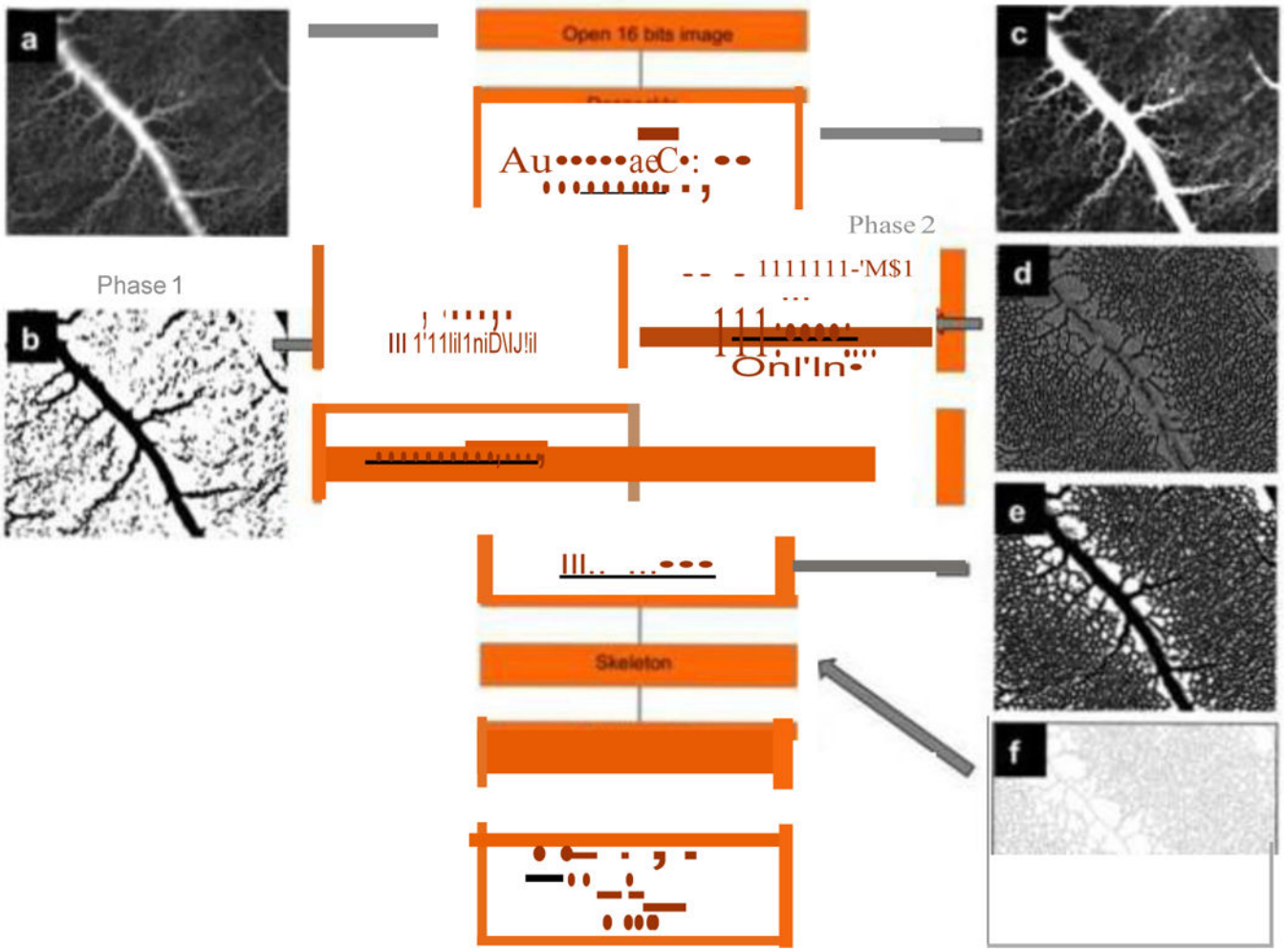

Figure 11.

Schematic representation of an image processing procedure used to characterize the CAM vascular network; **a** The original 16-bit image; **b** The same image after the **"**first phase**"** thresholding to extract main vessels; **c** The image after a posteriori shading correction filter; **d** The second parallel phase after the Laplacian filter; **e** The result after the conversion to an 8-bit image; **f** The result after the skeletonization process; **g** The corresponding histogram of non- vascularized meshes/mm^2 (surface distribution of non-vascularized regions). Adapted from [64].

Table 1

Advantages and disadvantages of the CAM model as a screening platform.

General biology
Advantages
- ease of use - feasibility of carrying out multiple tests on individual CAMs - rapid vascular growth - real-time visualization of the assays - complete accessibility to the circulatory system (for delivery of molecules intravascularly) - *in vivo* environment - excellent modeling of more complex systems - no requirement for animal protocol approval (country dependent)
Disadvantages
- chicken-origin of the assay limits availability of reagents - CAM itself is undergoing rapid changes both morphologically and in terms of the gradual change in the rate of endothelial cell proliferation during the course of embryonic development - immunodeficiency - contains a well-developed vascular network, which makes it difficult to discriminate between new capillaries and already existing ones - sensitive to environmental factors - differences in drug metabolism with mammals - shell dust (or other irritants) can induce angiogenesis
Methodology
Advantages
- monitoring throughout the course of the assay - rapid screening platform - accessibility to vessels of different caliber and types - reproducibility and reliability - cost-effectiveness
Disadvantages
- specie-related differences need to be taken into account in interpreting results obtained in experimental animals - complex choice of protocols available - alternative drug metabolism / pharmacokinetics when compared to other *in vivo* (mammalian) models - oral drug administration can not be tested - post grafting non-specific inflammatory reactions that my induce a secondary vasoproliferative response - short post-treatment observation time

Table 2

Broad applicability of the CAM in vascular assays.

Year	**Model**	**Ref.**
	In ovo	
1933	grafting; artificial air sac technique (NAST)	[15]
1956	tumor growth in the CAM and embryo	[16]
1956	“Zwilling-CAM”	[17]
2001	one-photon excitation PDT	[18–20]
2004	radiosensitizing activity	[21,22]
2004	experimental metastasis	[23]
2003	tissue engineering; “CAM cylinder model”	[24]
2003	angiogenesis	[25]
2006	angiogenesis	[26]
	Ex ovo	
1974	angiogenesis	[8]
1974	angiogenesis	[27]
1987	“artificial egg”; teratogenicity	[28]
2007	two-photon excitation photodynamic therapy (PDT)	[29]
2008	angiogenesis	[30]
2011	gene transfer / angiogenesis	[31]

Table 3

Imaging techniques used for the CAM and/or chicken embryo visualization.

Imaging technique	Ref.
optical doppler tomography (ODP)	[48]
laser doppler perfusion imaging	[49]
optical coherence tomography (OCT)	[50]
spectroscopic OCT combined with and speckle variance OCT	[50]
intravital videomicroscopy (IVVM)	[51, 52]
scanning electron microscopy (SEM)	[53]
magnetic resonance imaging (MRI)	[54]
positron emission tomography (PET)	[55]
fluorescent confocal microscopy	[56]
photoacoustic tomography (PAT)	[57]
biotinylated lipid-coated microbubble spectroscopy	[58]
optically sectioned fluorescence HiLo endomicroscopy	[59]
fractal analysis of arborization	[60]

Table 4

Summary quantification techniques to assess capillary networks.

Method	System	Descriptor	Ref.
Vessel level			
semi-quantitative	CAM vasculature	radius of the growth inhibition zone in 0–4 grades	[72,47]
quantitative	implanted collagen gels	vessel number growth vertically into the implanted collagen gels	[73,9]
semi-quantitative	Irritants applied topically on the CAM	vessel diameter	[74]
manual	Morphometric analysis	vessel diameter and length	[75]
semi-quantitative	fluorescent confocal microscopy	vessel density	[56]
automatic	developing/mature CAM	branching points/mm^2	[64] [62,69]
Capillary level			
semi-automatic	corrosion casting in scanning electron microscopy	capillary length, diameter, density	[76,77]
automatic	developing/mature CAM	branching points/mm^2	[64,19]
manual	post-fixation cross section analysis	number of capillary length	[78]

Table 5

Tumor cell lines and tumor tissue successfully used in the CAM to study tumor growth.

Type	Inoculation technique	Administration	Ref.
Tumor cell lines			
human ovarian carcinoma (A2780)	spheroid	topical	[39]
non-metastatic human colon carcinoma (SW480)	suspension serum-free medium	i.v.	[93]
human colorectal cancer (HTC-116)	matrigel	topical	[32]
human sarcoma (Saos-2 and SW1353)	matrigel		[94]
human clear cell renal cell carcinoma (CCRCC)	suspension in medium		[95]
osteosarcoma (various types)			[96]
murine melanoma B16-F10			[97]
human myeloma plasma cells	suspension in medium adsorbed on a gelatin sponge		[98]
head and neck squamous cell carcinoma (HNSCC) and peripheral blood mononuclear cells (PBMC) co-culture	cell culture insert		[99]
Tumor tissue			
Walker 256 carcinosarcoma	1–1.5 mm tissue fragments	allantoic cavity	[71]
human sarcoma	1–1.5 mm tissue fragments	topical	[94]
mouse teratoma, mouse C57 melanoma, rabit V2 carcinoma			[100]
meningioma, glioblastoma	lyophilized pieces		[101]
neuroblastoma	1–2 mm fragment		[101]
hepatocellular carcinoma	fragment		[102]
human M21-L melanoma, S100 melanoma	50 mg fragment		[103,104]
human ovarian adenocarcinoma	3–8 mm fragment		[105]
cryopreserved human ovarian adenocarcinoma	1–2 mm fragment		[106]

Table 6

Tumor cell lines shown to exhibit spontaneous cell intravasation, vasculotropism and metastasis in the CAM.

Cell type	Inoculation technique	Administration	Ref.
human neuroblastoma (IMR-32)	serum-free medium and matrigel	topical	[108]
human epidermoid carcinoma, human sarcoma, human embryonal rhabdomyosarcoma	explanted	subcutaneous	[16]
rat sarcoma	explanted	into the CAM	[92]
human epidermoid carcinoma (HEp-3)	suspension	topical	[109]
estrogen receptor negative (MDAMB231) and positive (MCF-7) breast adenocarcinoma			[109]
androgen receptor negative (PC3) and positive (LNCaP) prostate adenocarcinoma			[109]
human fibrosarcoma (HT-1080)			[109,93] [110]
human ovarian carcinoma (OVCAR-3, SKOV-3 and OV-90)			[111]
human embryo fibroblasts (HEF)			[109]
human colon carcinoma metastatic (SW620) and non-metastatic (SW480)	suspension in serum-free medium	i.v.	[93]
rat C6 glioma and 10AS pancreatic carcinoma	suspension in medium	topical	[83]
human Burkitt's lymphoma (BL)	matrigel		[112]

Table 7

Drug delivery systems tested on the CAM. PS: photosensitizer; AA: anti-angiogenic; A: angiogenic; AC: anti-cancer; AM: anti-microbial; ECs: endothelial cells; GF: growth factor; LF: lipid factor

	Delivery system	**Delivered drug**	**Ref**
immunoliposomes	coupled to a mAb targeting tumor cells (anti-GD2)	doxorubicin, AC	[125]
liposomes	Dipalmitoylphosphatidylcholine (DPPC)	meso-tetra(m-hydroxyphenyl)chlorin (PS)	[117]
(hydro)gels	amiloride	sucrose acetate isobutyrate (SAIB) and calcium alginate	[126]
	poly(ethylene glycol)-vinyl sulfone cross-linked with albumin	Spongosine 1-phosphate (S1P), LF	[127]
3D grafts type I fibrillar collagen	collagen onplants	GFs, A, AA	[30]
collagen matrices	collagen covalently linked with heparin	VEGF	[128]
conjugates with drugs	polyvinylpyrrolidone	PS	[129]
nanoparticles	poly(d,l-lactic acid)	meso(p-tetracarboxyphenyl)porphyri n (PS)	[130]
nanoparticles	poly (lactide-co-glycolide)	tetraiodothyroacetic acid	[131]
peptides	cell-penetrating peptides (bioportides)	peptides, proteins, and oligonucleotides	[132]
microspheres	poly (d,l-lactic acid)	taxol (AC)	[133]
microspheres	poly(epsilon-caprolactone)	paclitaxel (AC)	
filter disks	methylcellulose, nitrocellulose, Whatman paper	AA, PA, GF	[56]
pellets	ethylene-vinyl acetate (EVA) copolymer	-	[134]
liposomes	phosphatidylocholine	polyvinylpyrrolidone-iodine (AM)	[135]
scaffolds	poly(D,L-lactic) acid (PLA)	VEGF165, bFGF	[136, 137]
surface-engineered dendrimers	arginine conjugated poly(propylene)imine dendrimers	doxorubicin hydrochloride (AC)	[138]
bio-hydrogels	fibrin bio-hydrogel	genetically engineered cells over-expressing VEGF	[139]

Table 8

The CAM model in transplantations and tissue engineering studies.

System	Material	Ref.
transplants		
	chicken liver	[194, 197]
	human skin	[58, 179]
	chicken or quail embryos adrenal gland or cerebellum	[196]
	human proliferative endometrium	[195, 33]
	human ovarian tissue	[108, 109]
cells		
	murine embryonic stem cells (in gelatin-microbubble scaffold)	[198]
	mouse pulmonary stem/progenitor cells	[173]
	human dental pulp stem cells (in matrigel)	[176]
	rat nodose ganglion neurons	[199]
	human kidney-derived cells (in matrigel)	[174]
tissue-engineered matrices		
	human femoral cancellous bone chips	[84]
	chicken bone scaffolds	[200]
	bioactive glass ceramic scaffolds improving the growth and mineralization of skeletal components	[201]
	3D co-cultures of osteoblasts and ECs in DegraPol foam	[202]
	acetaminophen biosensors	[35]